Science
AAAS

Supplementary Materials for

Dome1–JAK–STAT signaling between parasite and host integrates vector immunity and development

Vipin S. Rana *et al*.

Corresponding author: Utpal Pal, upal@umd.edu

Science **379**, eabl3837 (2023)
DOI: 10.1126/science.abl3837

The PDF file includes:

Figs. S1 to S21
Tables S1 to S8

Other Supplementary Material for this manuscript includes the following:

MDAR Reproducibility Checklist

Fig. S1. Approach for the identification of the IFN-γ-binding tick protein

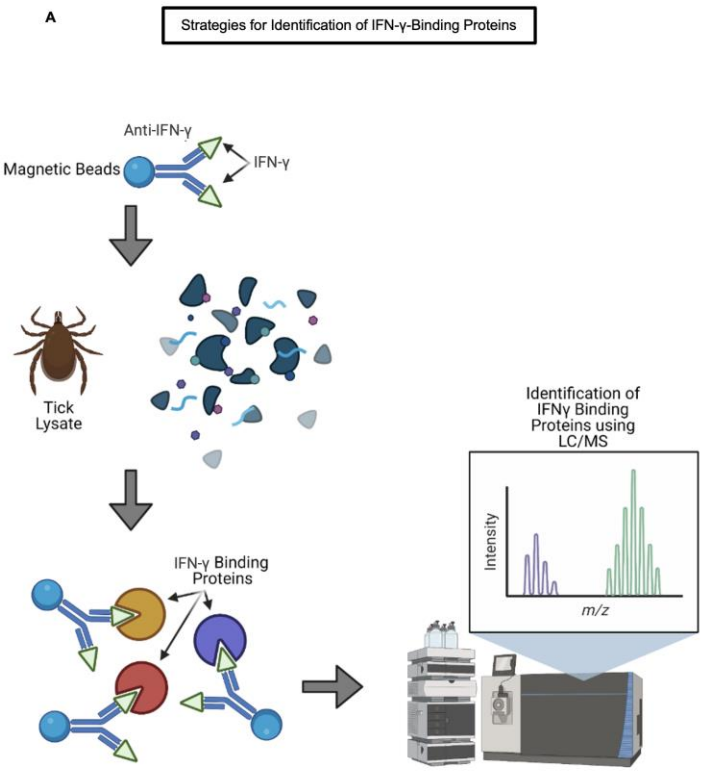

B

B7P6I6 (Dome1)

MHILNKTSLMVQGLTPYTNYTFRLRARASRAVMAELWTESVFLVQETLSDVPDSPPRISESGFK
VQNYQSKRSITLNFETVPRKHWCGAMLKYLVECCEENPLEDRCENKTSQVPTVTFENLLRNAA
YKFRLWSLNENGLSRVHSSMHVDRHDDLMNAPQDIKVMALSSGEYEVSWRPPATGRVLSGSS
PALSSGFEEAEAPSPGYTVFWCPRMLPRSYSCNQSLEWRRLPPNVTATLLQLEPDKVYQFAVA
AHGASNASEMAWTSCVIPVSKELEKITQVSLERDGPHSLLMRWQLECSALKSFVDGYQIEACAV
ADKYRNMALHDAADPRARGSISAELIGCQYSRYDPQSCKVYNVTNADAEERLLDGLDTNLVYR
AVVRALSNGRLTDDSPVQCARTESVGPAIS

Fig. S1. Approach for the identification of the IFN-γ-binding tick protein

(**A**) A schematic diagram showing the strategy for a co-immunoprecipitation assay using IFN-γ. Mouse recombinant IFN-γ was immobilized using Protein G Sepharose beads via rat anti-IFN-γ antibodies and incubated with whole tick lysates. After extensive washing, the proteins bound to IFN-γ were isolated and identified using a nano LC-MS/MS analysis. (**B**) Amino acid sequence of one of the IFN-γ-binding proteins, annotated as the cell adhesion molecule protein B7P6I6 and herein termed as Dome1, is shown. Two unique peptides (red font) of the Dome1 extracellular domain were identified via nano LC-MS/MS analysis (panel A). Results are representative of two independent experiments.

Fig. S2. Comparison of predicted structures and amino acid sequences of five Dome homologs from *Ixodes scapularis*

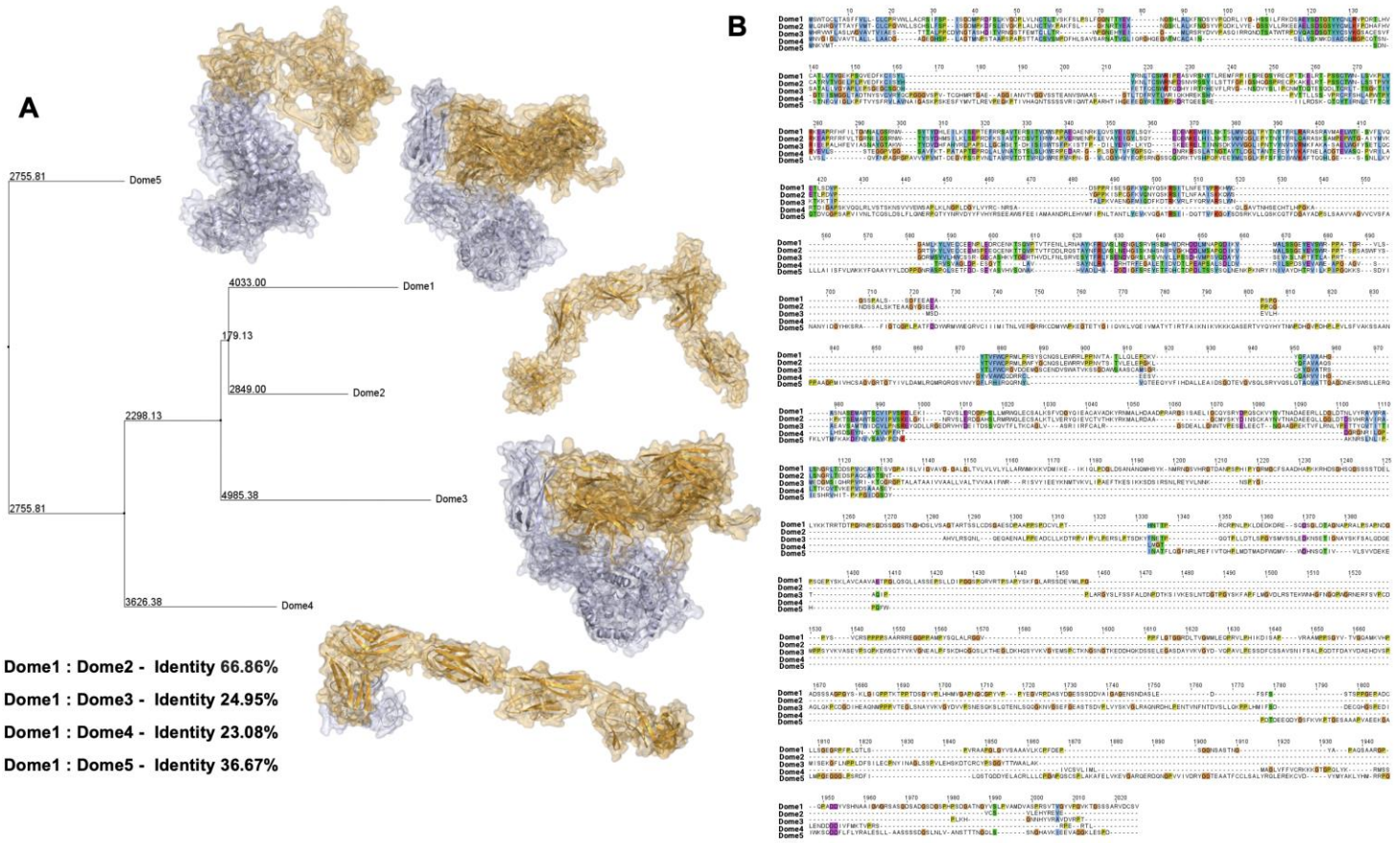

Fig. S2. Comparison of predicted structures and amino acid sequences of five Dome homologs from *Ixodes scapularis*

(**A**) A neighbor-joining phylogenetic tree, identity, and predicted structures showing the relationship of five *Ixodes* Dome proteins. The scale bar shows the approximate divergence in amino acid changes per residue. (**B**) The amino acid sequence homology between Dome homologs from *I. scapularis.* Amino acids with similar properties are labeled with identical colors.

Fig. S3. Phylogenetic analyses of Dome1

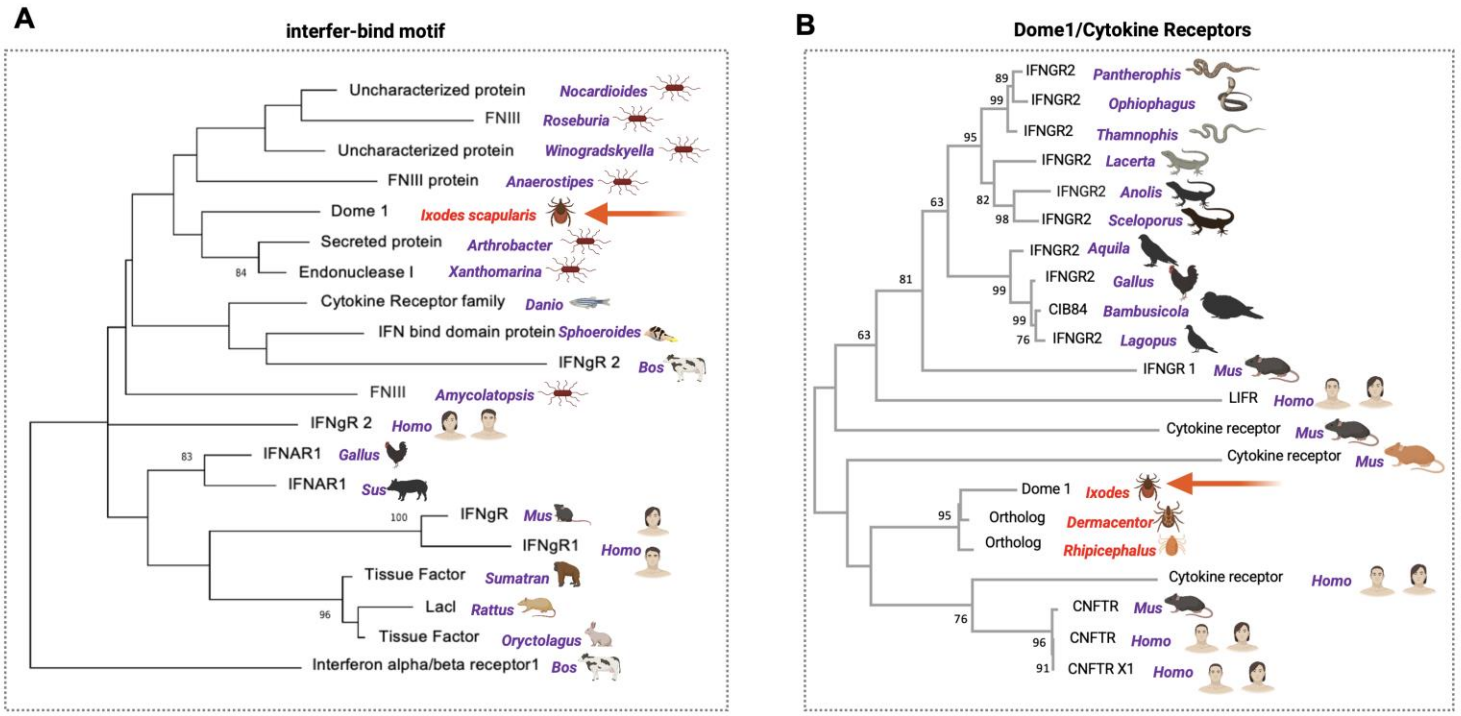

Fig. S3. Phylogenetic analyses of Dome1

(**A**) Occurrence of mammalian interfer-bind motif in proteins of several bacterial and animal species and *Ixodes* Dome1. The comparative sequence analysis of interfer-bind motif revealed its close match to several bacterial and animal proteins, and Dome1. A maximum likelihood phylogenetic tree was generated using interfer-bind motif from various bacterial and animal species. Branch support values greater than 0.7 are indicated by numbers. Note that bacterial genera, such as *Roseburia*, are known to be present in wild-caught *I. scapularis* ticks. (**B**) The comparative sequence analysis of vertebrate cytokine receptors revealed a close match to Dome1. A maximum likelihood phylogenetic tree was generated using available sequences for various cytokine receptors from selected reptilian, avian, and mammalian genomes and representative tick Dome proteins.

Fig. S4. Purification of Dome1 protein and generation of polyclonal antibodies

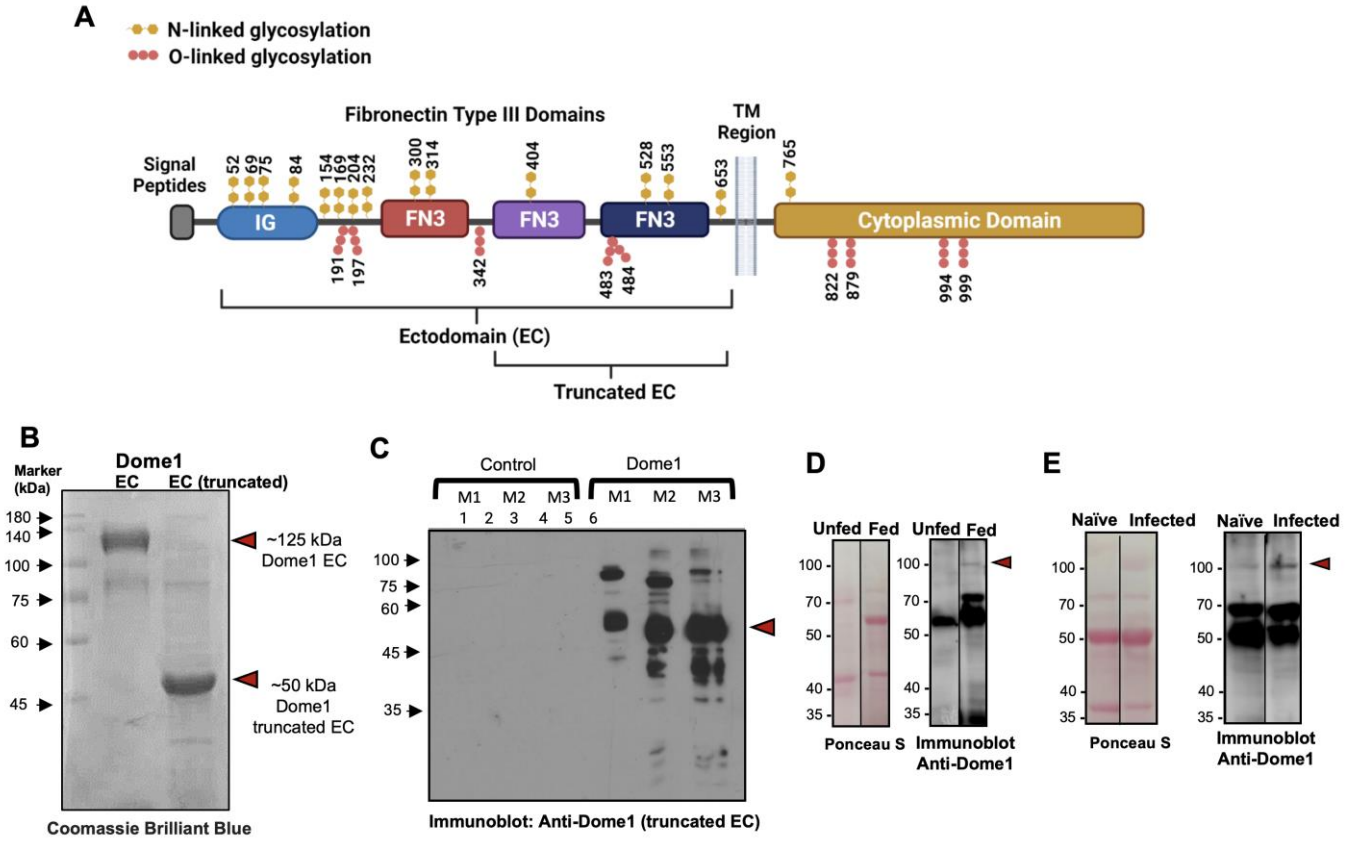

Fig. S4. Purification of Dome1 protein and generation of polyclonal antibodies

(**A**) Schematic representation of Dome1 showing glycosylation sites and regions that were targeted for the production of recombinant Dome1 proteins. The entire non-cytoplasmic/ extracellular domain (Ectodomain, EC), ~125 kDa, was cloned and expressed in a mammalian (CHO cell) expression system, while smaller regions like (truncated EC), ~50 kDa, was produced using a bacterial (*E. coli*) expression system. (**B**) Purified His-tagged recombinant Dome1 proteins (EC and truncated EC, arrows). The proteins were resolved using 12% SDS-PAGE gel and stained with Coomassie Brilliant Blue. (**C**) Generation of murine polyclonal anti-Dome1 antibodies. Groups of mice were immunized with recombinant Dome1 (truncated EC), and their serum was analyzed for the presence of anti-Dome1 antibodies. Lanes 1-3 represent individual control mice immunized with PBS and adjuvant, while lanes 4-6 represent mice immunized with Dome1; antibodies against ~50 kDa truncated EC Dome1 is indicated by an arrowhead. (**D**) Detection of Dome1 in *I. scapularis* nymphs. Antibody against Dome1 (panel C) was used to detect Dome1 expressed in unfed and 48-hour-fed nymphs (arrowhead), while total protein profile is shown by staining with Ponceau S. (**E**) Enhanced Dome1 production in *B. burgdorferi*-infected fed nymphs. Nymphal tick lysates (3 ticks per group) were prepared from separate groups of 48-hour-fed ticks that fed either on naïve C3H mice or a parallel group of mice that were infected with *B. burgdorferi* for two weeks. Comparable protein levels were shown by staining with Ponceau S, with Dome1 indicated by arrowhead.

Fig. S5. ***Anaplasma phagocytophilum*** **infection does not trigger JAK–STAT signaling and Dae2 antimicrobial responses in** ***I. scapularis*** **ticks**

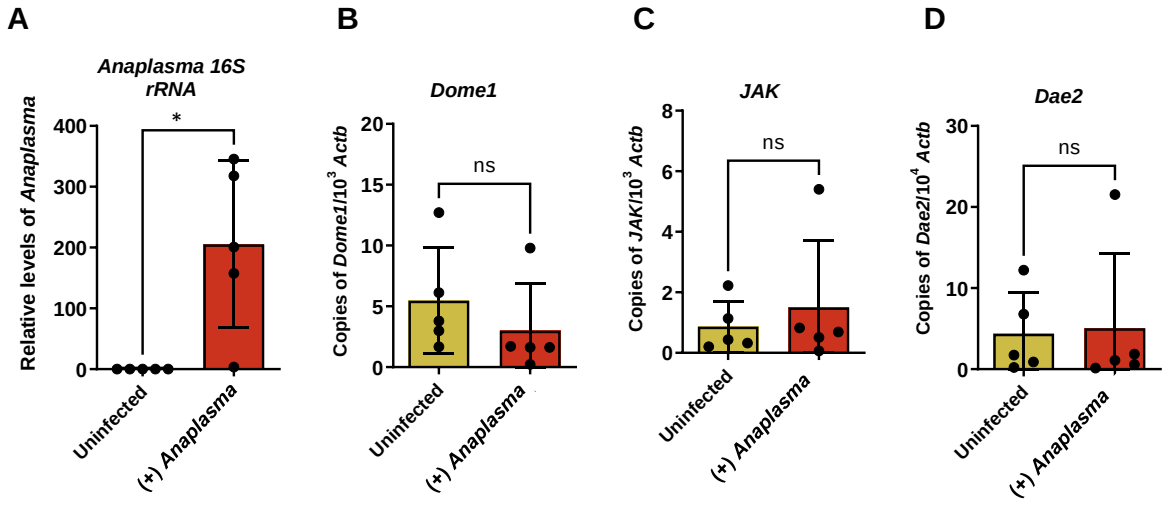

Fig. S5. *Anaplasma phagocytophilum* infection does not trigger JAK–STAT signaling and Dae2 antimicrobial responses in *I. scapularis* ticks

Groups of nymphs were allowed to feed on naïve or *A. phagocytophilum*-infected mice and were then analyzed for the induction of Dome1 and the JAK–STAT pathway. (**A**) The presence of *A. phagocytophilum* in infected nymphs. Nymphs that fed on naïve or infected mice were processed for qPCR using pathogen-specific 16S rRNA primers. *A. phagocytophilum*-specific signals were undetectable when feeding on uninfected mice, but were detectable in the group that parasitized infected mice. (**B to D**) The transcript levels of *Dome1* (panel B), *JAK* (panel C), and *Dae2* (D) were analyzed in naïve and *Anaplasma*-infected tick guts (5 nymphs per group) using RT-qPCR and gene-specific primers. The mRNA levels for all genes in naïve or *A. phagocytophilum*-infected ticks were statistically non-significant (ns). Data are presented as mean ± SD; n = 5; **P*<0.05, determined using two-tailed Mann–Whitney *U* test.

Fig. S6. IFN-γ and *Dome1* deficiency in murine blood and tick organs

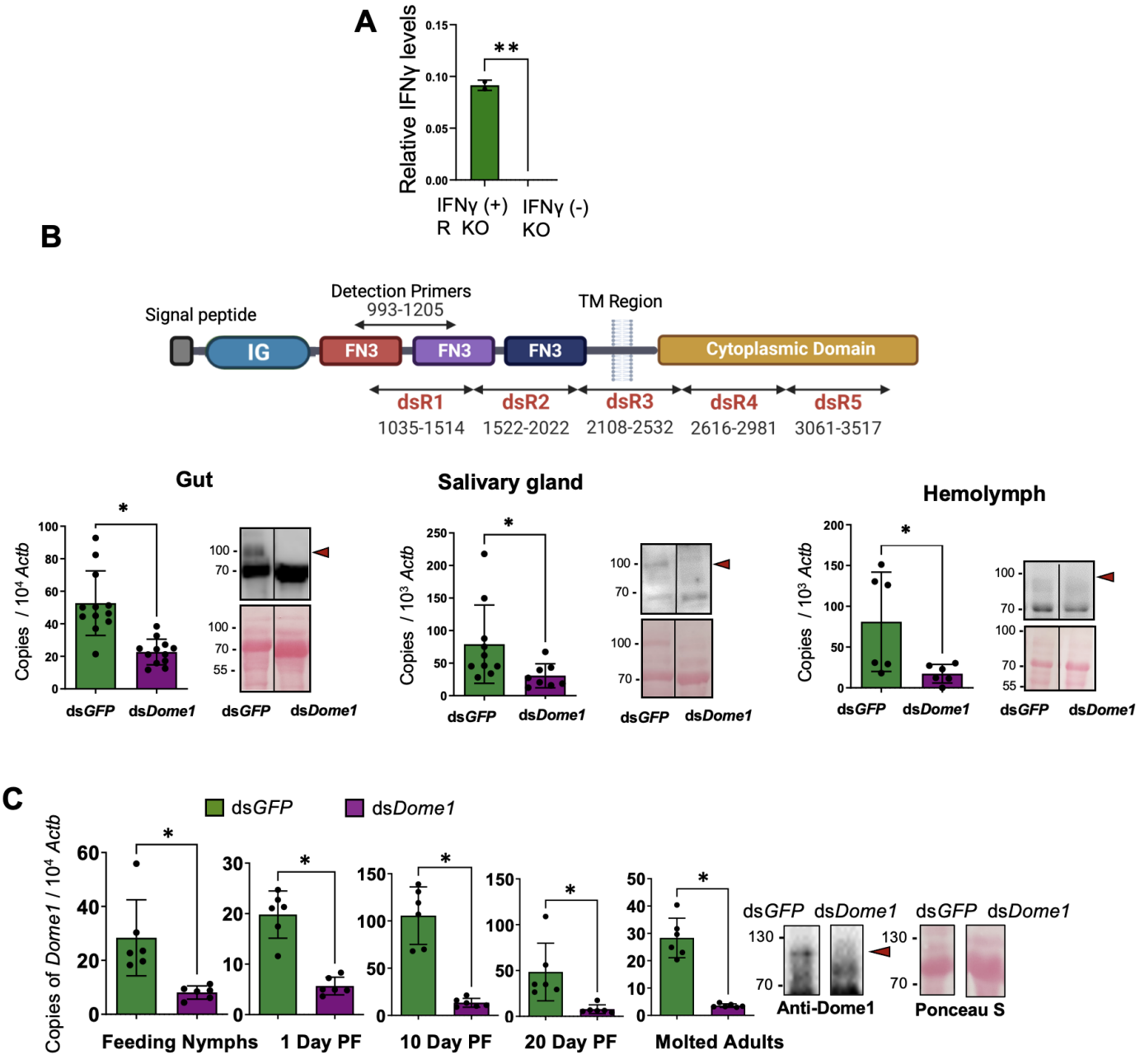

Fig. S6. IFN-γ and *Dome1* deficiency in murine blood and tick organs

(**A**) Lack of IFN-γ in blood sample of *Ifngr1*-knockout mice, as detected by standard ELISA. ***P*<0.05, determined using two-tailed Student's *t* test. (**B**) *Dome1* expression and its silencing via RNA interference (RNAi). The upper panel shows a schematic representation of the *Dome1* open reading frame, showing regions targeted for RNAi. The lower panel represents *Dome1* knockdown in multiple nymphal tick organs. Separate groups of ticks were microinjected with dsRNA targeting *GFP* or *Dome1* and then placed on naïve C3H mice for 48 hours. The partially fed ticks were collected from mice and dissected for hemolymph, salivary gland, and gut samples. The levels of *Dome1* transcripts and protein in all three organs were quantified via RT-qPCR by using *Dome1* primers and normalizing against transcripts of tick *β-actin* (*Actb*) levels, and by western blotting using Dome1 antibodies (arrows, adjacent panels). Significant downregulation of *Dome1* transcripts was observed in the tested organs of *Dome1*-knockdown ticks. The experiments were repeated three times and each dot represents the pool of tissue samples collected from at least three ticks. (**C**) Transstadial maintenance of RNAi-mediated Dome1 knockdown in nymphs throughout tick feeding (48 hours), post-fed (PF) intermolt periods, and adult stage. The rightmost panels show the knockdown of Dome1 protein levels in adult tick gut samples (arrowheads). Results are representative of two to three independent experiments (n = 6-10); **P*<0.05, determined using two-tailed Mann–Whitney *U* test.

Fig. S7. Impact of *Dome1* knockdown on expression of other *Dome* homologs

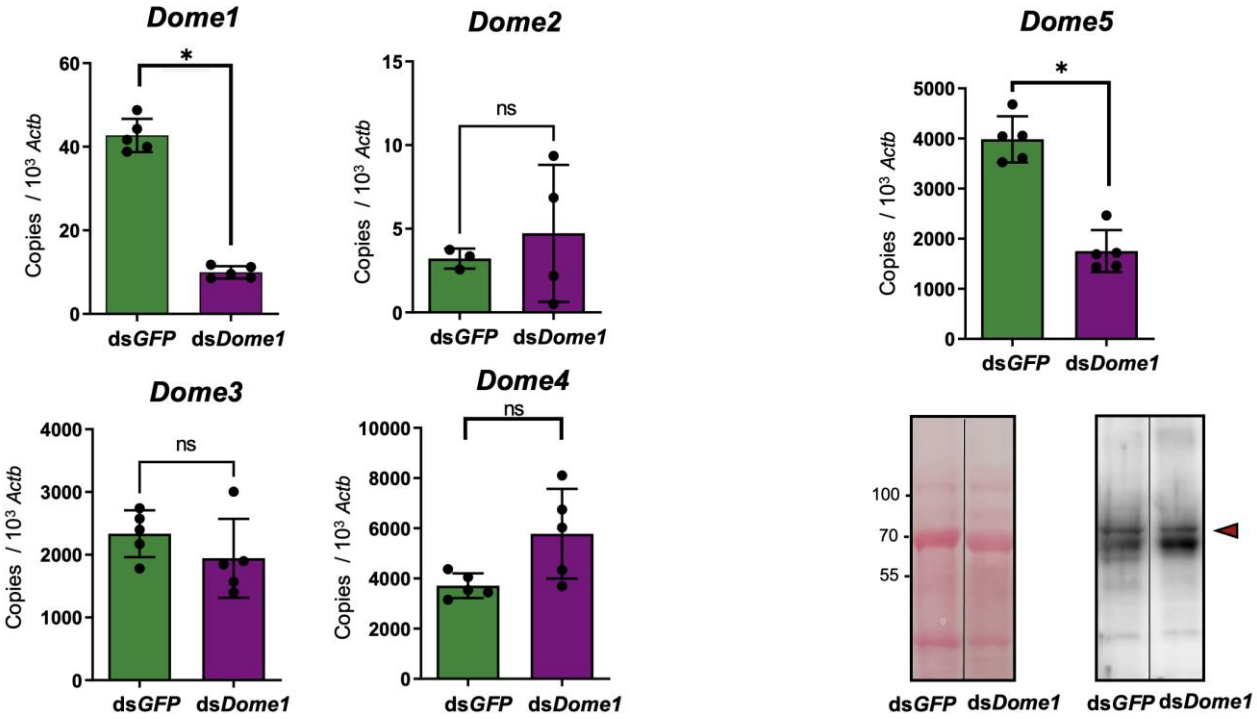

Fig. S7. Impact of *Dome1* knockdown on expression of other *Dome* homologs

The expression of *Dome2*, *Dome3*, *Dome4*, and *Dome5* were analyzed in *Dome1*-knockdown ticks via RT-qPCR. Nymphs were microinjected with dsRNA targeting either *GFP* or *Dome1* and were placed on naïve C3H mice for 48 hours. The partially fed ticks were collected from mice and analyzed for the expression of all *Dome* homologs. Notably, except for *Dome5*, no significant variations were observed in the expression of *Dome2*, *Dome3*, and *Dome4*. The lower right panel denotes the detection of Dome5 protein in 48-hour-fed *I. scapularis* nymphs. Gut samples from *Dome1*-knockdown or control ticks were immunoblotted using antibody generated against recombinant Dome5 (fig. S9). The arrowhead denotes the position of native Dome5 in ticks. The total protein profile in the tick gut is shown by Ponceau S staining. Results are representative of two to three independent experiments. Quantitative data are shown as individual data points and means ± SDs (n = 5). $*P<0.05$, determined using two-tailed Mann–Whitney *U* test; ns, non-significant.

Fig. S8. *Dome1* deficiency alters homeostasis of reactive oxygen species in feeding ticks

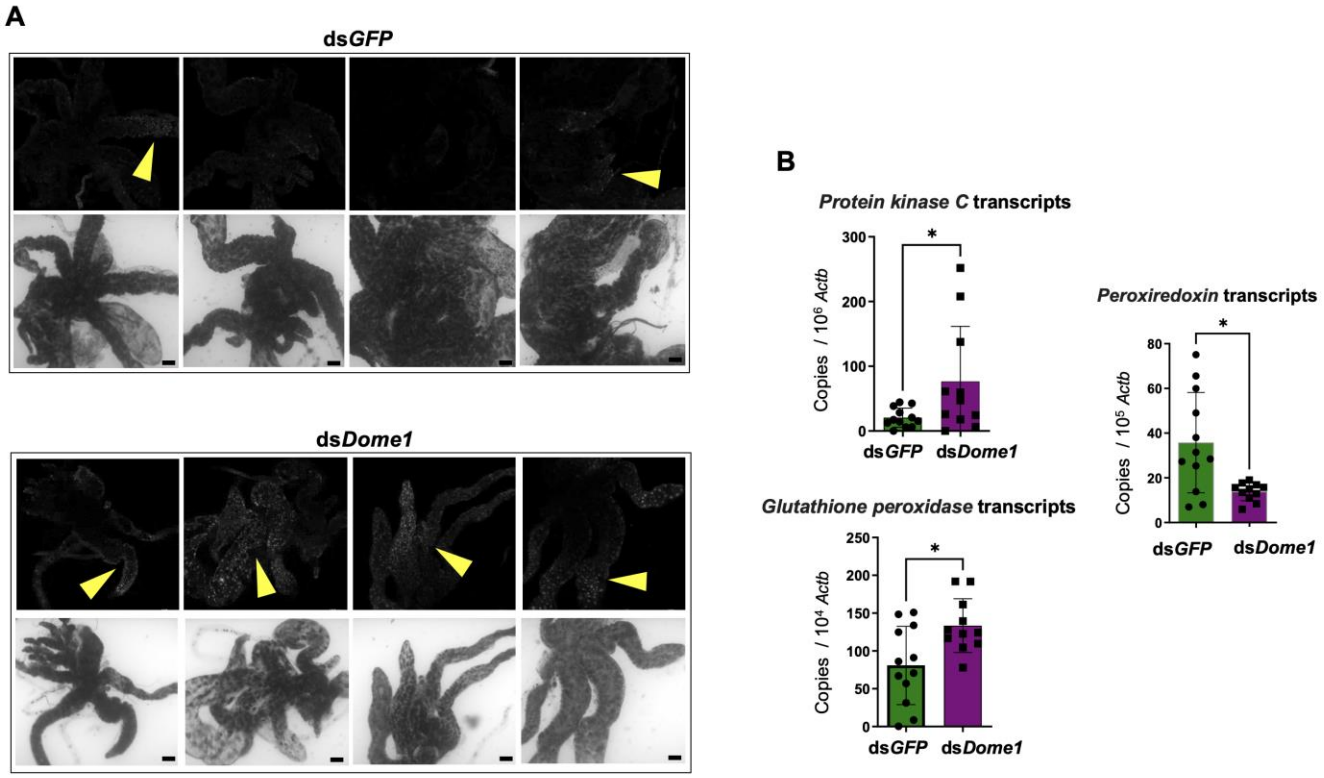

Fig. S8. *Dome1* deficiency alters homeostasis of reactive oxygen species in feeding ticks

Separate groups of nymphs (25 ticks per group) were microinjected with ds*Dome1* or control ds*GFP* RNA (4 µg/µl) and then fed on *B. burgdorferi*-infected mice for 48 hours. (**A**) The dissected gut samples from partially fed ticks were processed for the detection of ROS using dihydroethidium reagent (DHE), which detects superoxide radicals. Once oxidized, DHE intercalates into DNA and fluoresces red (presented in a gray scale). A higher level of ROS production was observed in *Dome1*-knockdown ticks (arrows), as assessed via confocal immunofluorescence microscopy. Scale bar = 100 µm. (**B**) The expression profiles of a few representative genes associated with ROS homeostasis, including *protein kinase C*, *peroxiredoxin*, and *glutathione peroxidase*, were compared in ticks microinjected with ds*Dome1* or control ds*GFP*. The expression levels of target genes were normalized against tick *Actb* levels. Results are representative of two to three independent experiments. Quantitative data are shown as individual data points and means ± SDs (n = 6 to 10). **P*<0.05, determined using two-tailed Mann–Whitney *U* test.

Fig. S9. RNAi-mediated knockdown of *Dome5* has no effect on JAK–STAT signaling, *B. burgdorferi* colonization, or tick metamorphosis

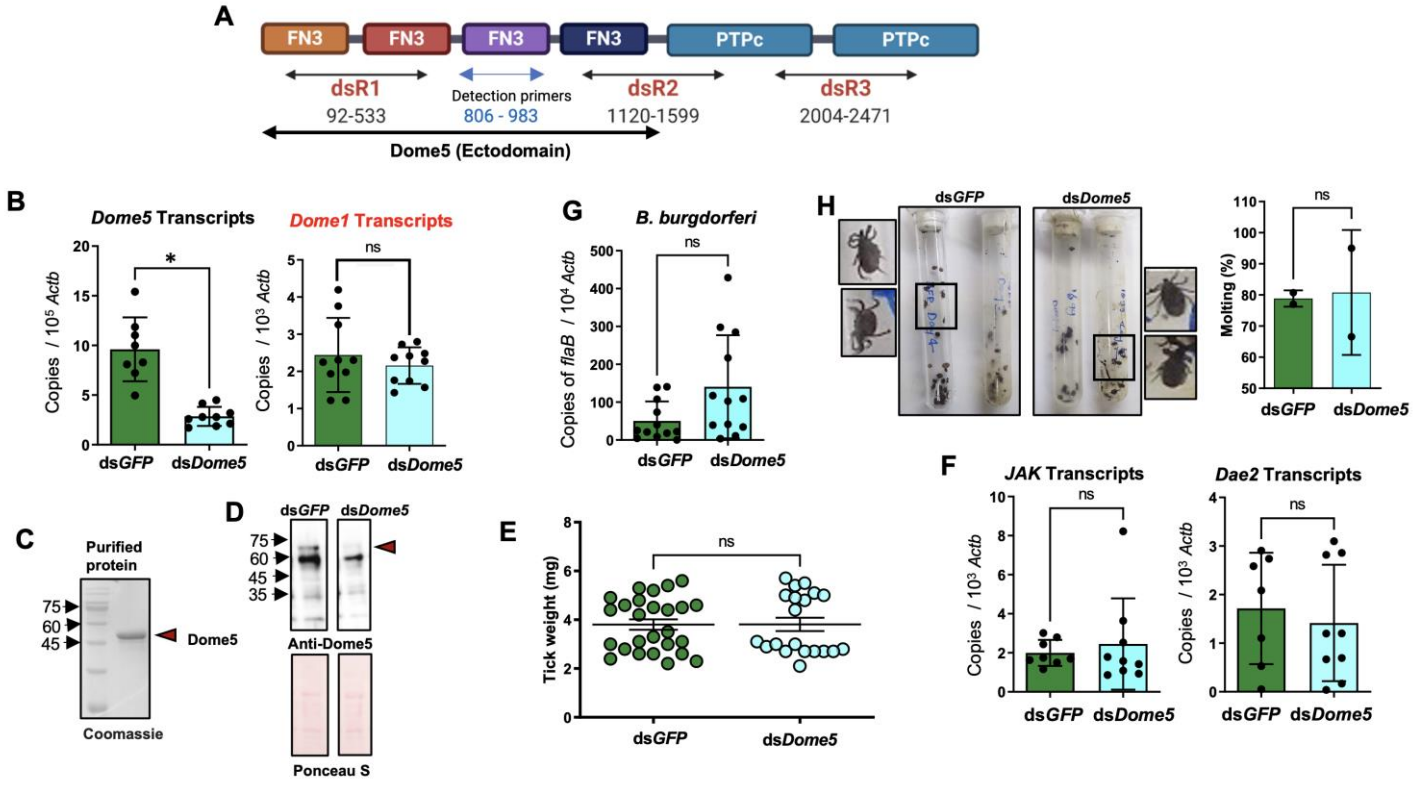

Fig. S9. RNAi-mediated knockdown of *Dome5* has no effect on JAK–STAT signaling, *B. burgdorferi* colonization, or tick metamorphosis

(**A**) Schematic representation of the *Dome5* open reading frame, showing regions targeted for RNAi. The regions encompassing dsRNA constructs (ds*R1*-ds*R3*) and detection primers are shown. A pool of ds*R1-R3* RNA was used to knock down *Dome5*. (**B**) The knockdown of *Dome5* in nymphal ticks. Nymphs (20 ticks per group) were microinjected with ds*Dome5* or control ds*GFP* RNA (4 µg/µl) and then fed on *B. burgdorferi*-infected mice for 48 hours. The partially fed ticks were processed for *Dome5* and *Dome1* mRNA levels using specific primers and normalizing against tick *Actb* levels. (**C**) Purified recombinant Dome5 protein (arrow), which was used to generate polyclonal antibodies in mice. (**D**) Detection of native Dome5 in *Dome5*-knockdown ticks. The gut samples from 48-hour-fed *Dome5*-knockdown or control ticks, as detailed in panel B, were analyzed by immunoblotting using anti-Dome5 antibodies. Equal protein loading is indicated by Ponceau S (lower panels). (**E**) *Dome5* silencing did not impact tick feeding. The engorgement weights of fed ticks are indicated. (**F**) *Dome5* knockdown had no effects on the JAK–STAT pathway and associated antimicrobial responses. *Dome5*-knockdown or control ticks were assessed for transcript levels of *JAK* and *Dae2* by RT-qPCR. (**G**) Knockdown of *Dome5* did not influence the colonization of *B. burgdorferi* within the tick gut. The spirochete burden in 48-hour-fed ticks was assessed via measuring *flaB* transcripts and normalizing to tick *Actb* using RT-qPCR. (**H**) Dome5 function is not associated with tick molting, as seen in representative images of molted ticks (left panel) and its quantitative presentation (right panel). Results are representative of two to three independent experiments. Quantitative data are shown as individual data points and means ± SDs (n = 8 to 26). $*P<0.05$, determined using two-tailed Mann–Whitney U test; ns, non-significant.

Fig. S10. Scanning electron micrographs of knockdown ticks

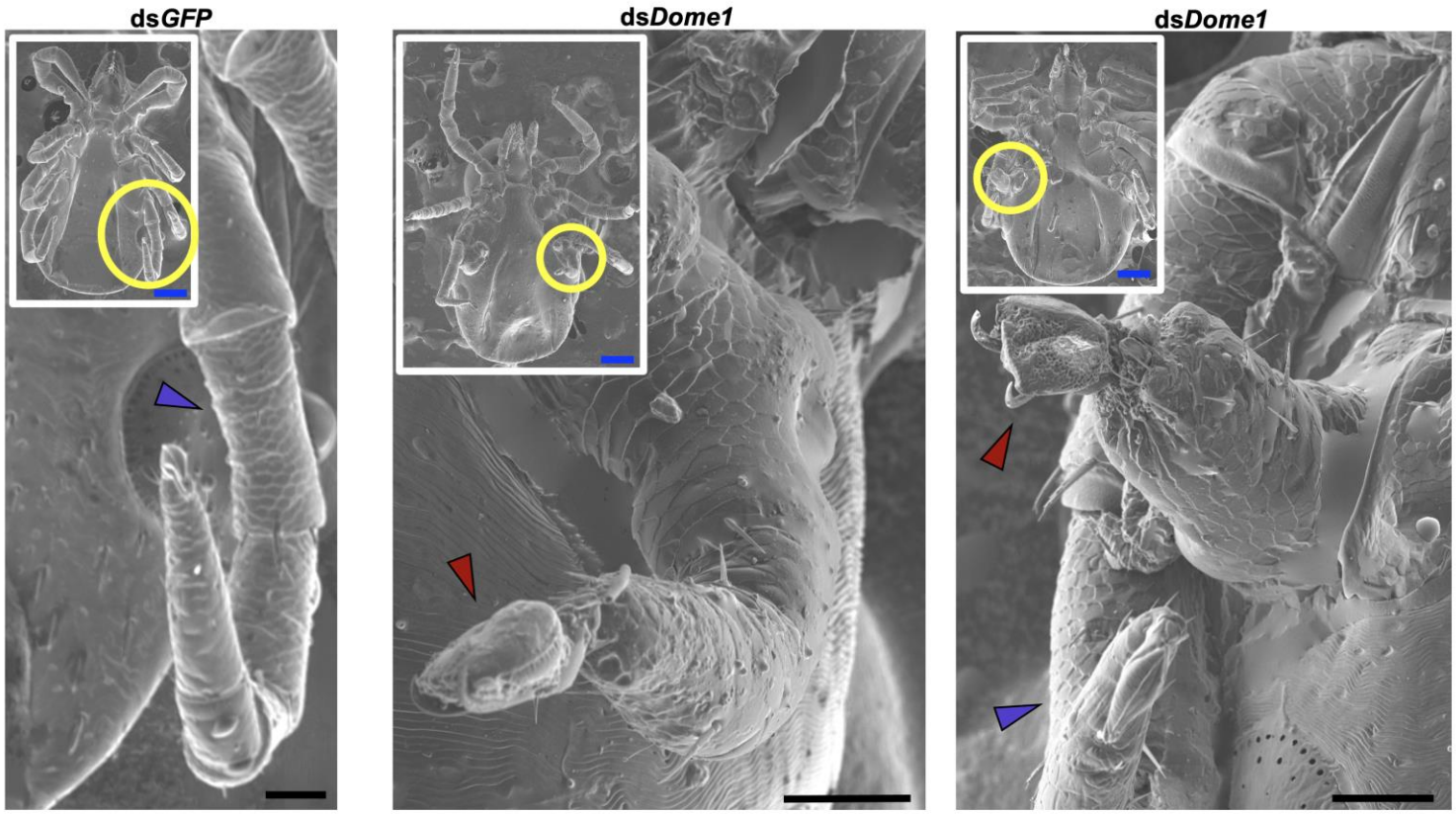

Fig. S10. Scanning electron micrographs of knockdown ticks

Engorged larvae were microinjected with *Dome1* or control (*GFP*) dsRNA and analyzed for phenotypic variations in newly molted nymphs. The insets show the whole ticks, and the yellow circles correspond to the highly magnified views of normal legs (blue arrowheads) or malformed legs in *Dome1*-knockdown ticks (red arrows). Results are representative of three independent experiments. Black scale bar = 50 µm, blue scale bar = 200 µm.

Fig. S11. Dome1 is essential for fecundity and early larval development

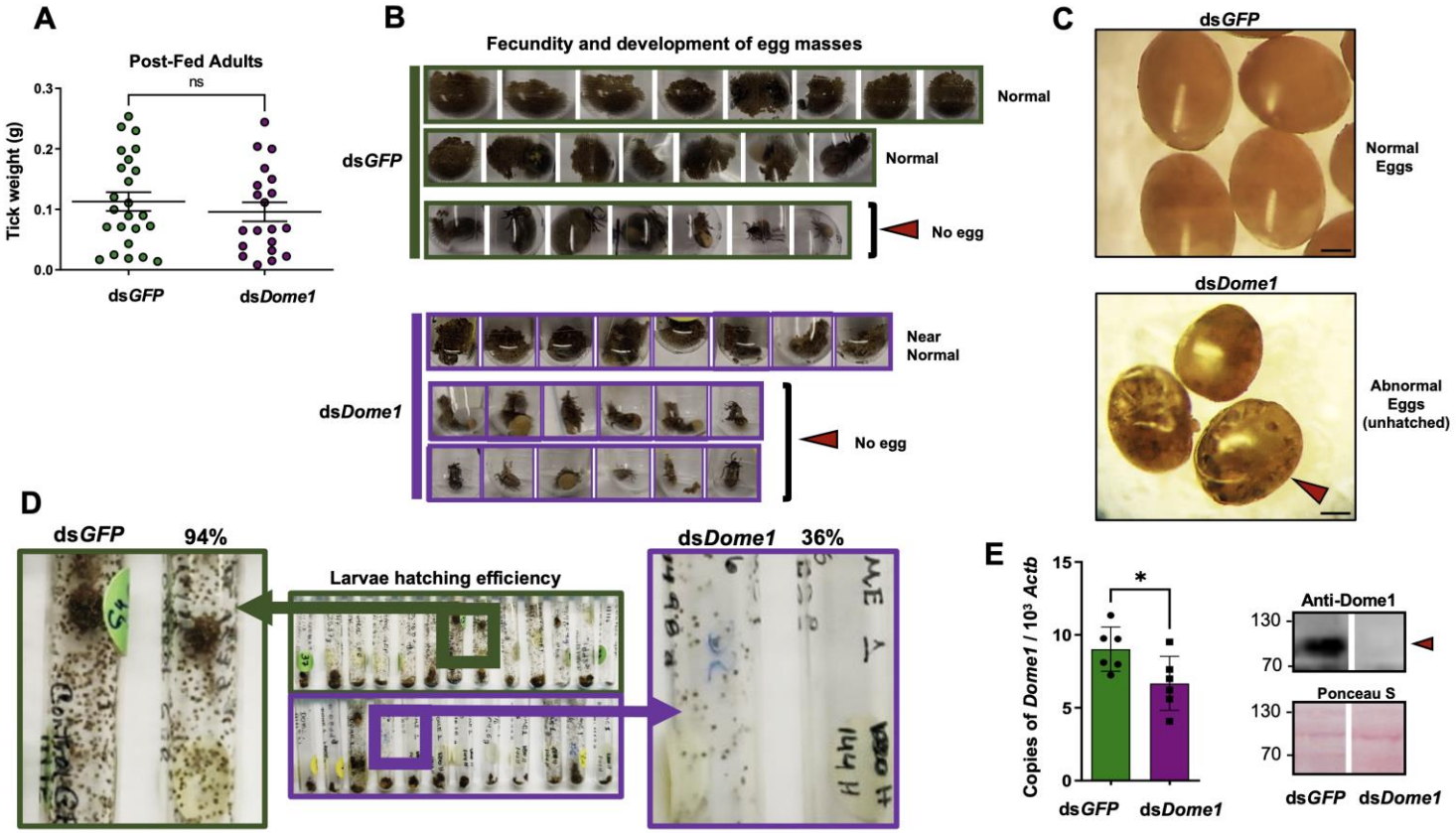

Fig. S11. Dome1 is essential for fecundity and early larval development

Adult females of *I. scapularis* (25 ticks per group) were microinjected with ds*Dome1* or ds*GFP* (control) RNA and allowed to engorge on separate groups of rabbits. (**A**) Knockdown of *Dome1* did not influence optimal tick engorgement. Ticks were weighed immediately after feeding to repletion, with no significant difference recorded between *Dome1*-deficient or control groups. (**B**) *Dome1* deficiency impacts fecundity and development of egg masses. While most of the egg masses from the control ticks had normal anatomical features, many of the *Dome1*-deficient ticks were unable to lay eggs (arrow) or yielded smaller egg masses. (**C**) Abnormal egg development in *Dome1*-knockdown ticks. In contrast to the normal morphological features of the eggs laid by control (ds*GFP*-injected) ticks (upper panel), the *Dome1*-deficient females generated eggs with abnormal features (lower panel), most of which remain unhatched (arrow). Scale bar = 20 µm. (**D**) *Dome1* deficiency impairs optimal egg hatching and larval emergence. Most of the eggs laid by control ticks (94%) gave rise to larvae (left panel); however, larval emergence was recorded from a smaller fraction (36%) of the eggs from the *Dome1*-knockdown females (right panel). (**E**) Knockdown of *Dome1* sustained in newly hatched larvae. The emerged larval masses were processed for *Dome1* mRNA or protein levels by RT-qPCR (left panel) or western blot analyses using anti-Dome1 antibodies (right panels), respectively. Lower levels of *Dome1* transcripts or Dome1 protein (red arrow) were observed in the larvae of *Dome1*-knockdown female ticks, as compared to control ticks. Quantitative data are shown as individual data points and means ± SDs (n = 6 to 23). **P*<0.05, determined using two-tailed Mann–Whitney *U* test; ns, non-significant.

Fig. S12. RNAi-mediated knockdown of *Dome1*, *JAK*, and *STAT* in larval ticks yields comparable developmental defects in newly molted nymphs, impacting blood meal engorgement of *B. burgdorferi*-infected ticks and spirochete transmission.

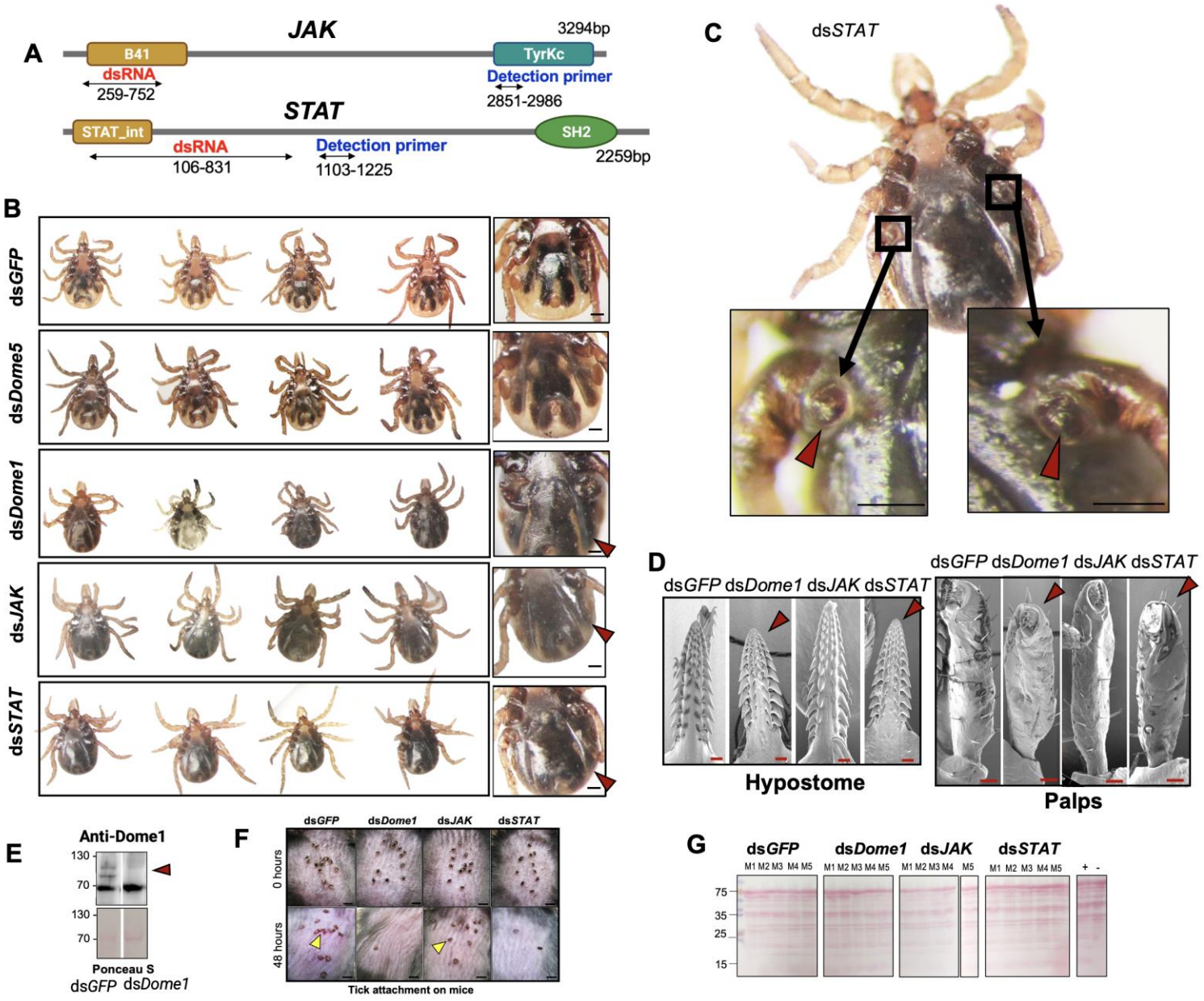

Fig. S12. RNAi-mediated knockdown of *Dome1*, *JAK*, and *STAT* in larval ticks yields comparable developmental defects in newly molted nymphs, impacting blood-meal engorgement of *B. burgdorferi*-infected ticks and spirochete transmission.

(**A**) Schematic representation of the *JAK* and *STAT* open reading frames, showing regions targeted for RNAi. Detection primers were used for the assessment of transcript silencing using RT-qPCR. Abbreviations: B41, Band 4.1 homolog; TyrKc, tyrosine kinase catalytic domain; STAT_int, protein interaction domain; SH2, Src homology 2 domain. (**B**) Separate groups of fed larvae were microinjected with ds*Dome1,* ds*JAK,* or ds*STAT*; control ticks were microinjected with either ds*GFP* or ds*Dome5* RNA. The larvae were allowed to molt and were then analyzed as newly molted unfed nymphs. Viable ticks were imaged under a dissecting binocular microscope, which showed comparable developmental defects, including darker abdomens (arrows), in *Dome1*-, *JAK*-, or *STAT*-knockdown ticks, while the control *Dome5*-knockdown or ds*GFP*-injected nymphs had normal appearances. (**C**) A representative *STAT*-knockdown tick showing an additional defect of rudimentary legs (arrow). Scale bar = 50 µm. (**D**) Close-up view of the morphological defects highlighted in Fig. 3, indicating shorter hypostome and pulps in ds*Dome1* and ds*STAT* groups (arrowheads), as compared to controls (*dsGFP*). (**E**) (A) Transstadial knockdown of *Dome1*, *JAK*, and *STAT* in infected unfed nymphs. Larvae that had engorged on *B. burgdorferi*-infected mice were microinjected with target dsRNA and allowed to molt. Reduced Dome1 levels (arrowhead) were observed in knockdown ticks, as assessed by immunoblotting. (**F**) Attachment of knockdown ticks on mice during spirochete transmission, as detailed in Fig 8. Nymphs (12 ticks per group) were allowed to engorge on naïve mice (scale bar = 1 mm). Tick attachment was observed at various time points until repletion. (**G**) Equal protein loading, as assessed by Ponceau S, are shown for the representative immunoblot shown in Fig. 8G. Results are representative of two to three independent experiments.

Fig. S13. Suppression of *I. scapularis* JAK–STAT pathway impacts tick metamorphosis and gut homeostasis

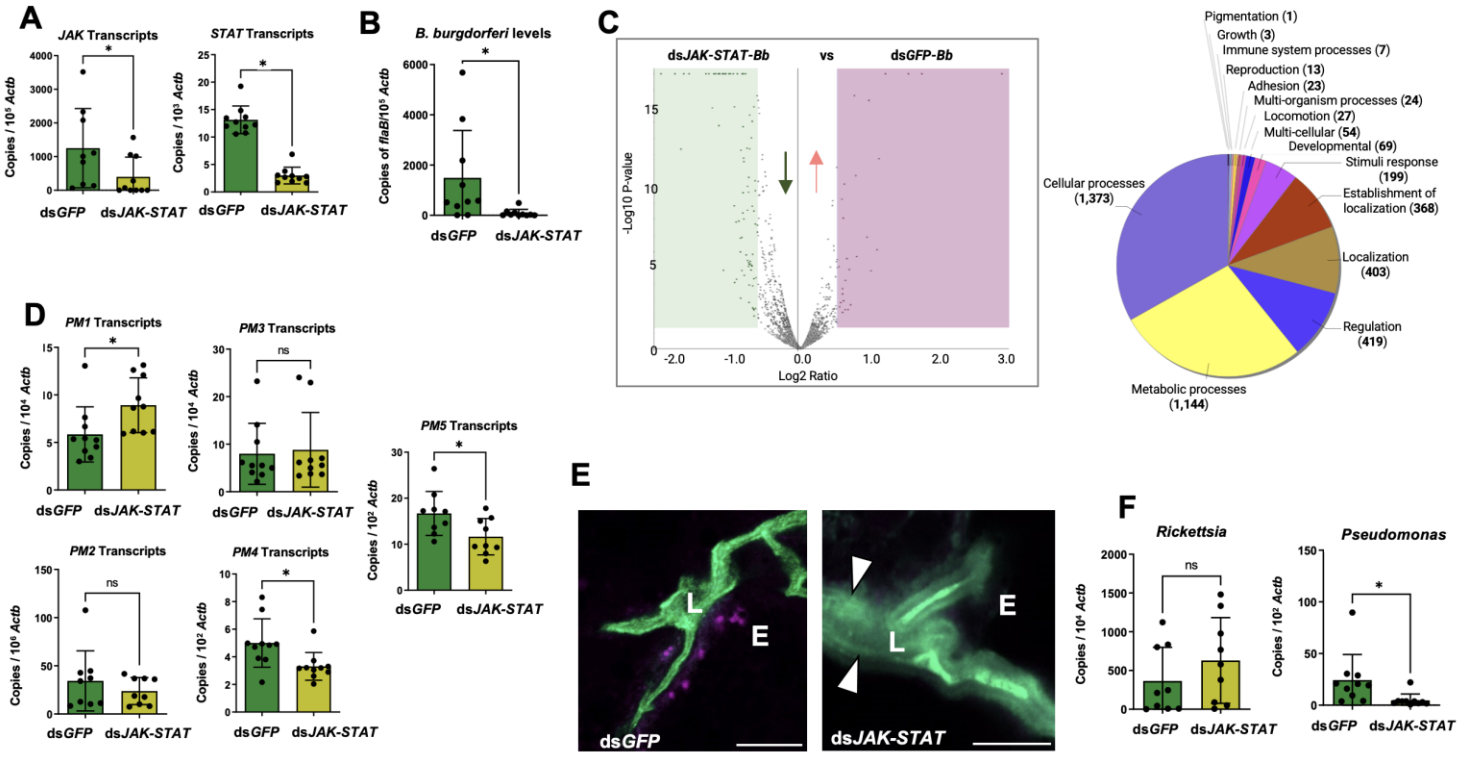

Fig. S13. Suppression of *I. scapularis* JAK–STAT pathway impacts tick metamorphosis and gut homeostasis

(**A**) Simultaneous knockdown of *JAK* and *STAT* expression by RNAi in nymphal ticks. Separate groups of nymphs (20 ticks per group) were microinjected with ds*JAK* and ds*STAT* (ds*JAK-STAT*) or control ds*GFP* RNA (4 µg/µl) and then fed on naive mice for 48 hours. The partially fed ticks were processed for *JAK* and *STAT* mRNA levels using specific primers and normalizing against tick *Actb* levels. (**B**) Suppression of JAK–STAT pathway impairs the colonization of *B. burgdorferi* within the tick gut. Dissected guts from nymphs that had partially engorged on *B. burgdorferi*-infected C3H mice were processed for RT-qPCR via measuring *flaB* transcripts and normalizing to tick *Actb*. (**C**) Differential production of gut proteins in *JAK–STAT*-knockdown ticks. Sets of proteins that are significantly up- or downregulated in *JAK–STAT*-knockdown ticks were identified using isobaric tandem mass tag (TMT) multiplexed quantitative proteomics. The most dramatically up- or downregulated proteins are indicated by the shaded purple or green areas, respectively (left panel). The number of identified proteins involved in predicted biological processes are indicated by the pie chart (right panel). (**D**) Suppression of JAK–STAT pathway alters expression of peritrophin genes, including *PM5*. The mRNA levels of five peritrophins were analyzed by RT-qPCR in 48-hour-fed ticks. (**E**) Alteration of peritrophic matrix (PM) permeability in *JAK–STAT*-knockdown ticks. Confocal microscopy was performed to analyze 48-hour-fed nymph guts (previously microinjected with ds*JAK-STAT* or ds*GFP* RNA) that were capillary fed with fluorescein-conjugated 500,000 (green) and rhodamine red-conjugated 10,000 (violet) MW dextran molecules. While the PM was impermeable to high molecular weight dextran beads, which were confined within the lumen of control ticks, the beads crossed the PM barrier and endocytosed inside some gut epithelial cells in *JAK–STAT*-

knockdown ticks (arrows). L, lumen; E, epithelial cells. Scale bar = 10 μm. (**F**) *JAK–STAT*-knockdown alters selected microbial species in ticks. *JAK–STAT*-knockdown or control (ds*GFP*) ticks were allowed to partially engorge on *B. burgdorferi*-infected mice. Nymphal guts were analyzed via RT-qPCR targeting selected microbial species. Quantitative data are shown as individual data points and means ± SDs (n = 3 to 9). **P*<0.05, determined using two-tailed Mann–Whitney *U* test; ns, non-significant.

Fig. S14. Host IFN-γ influences cell proliferation in nymphal gut

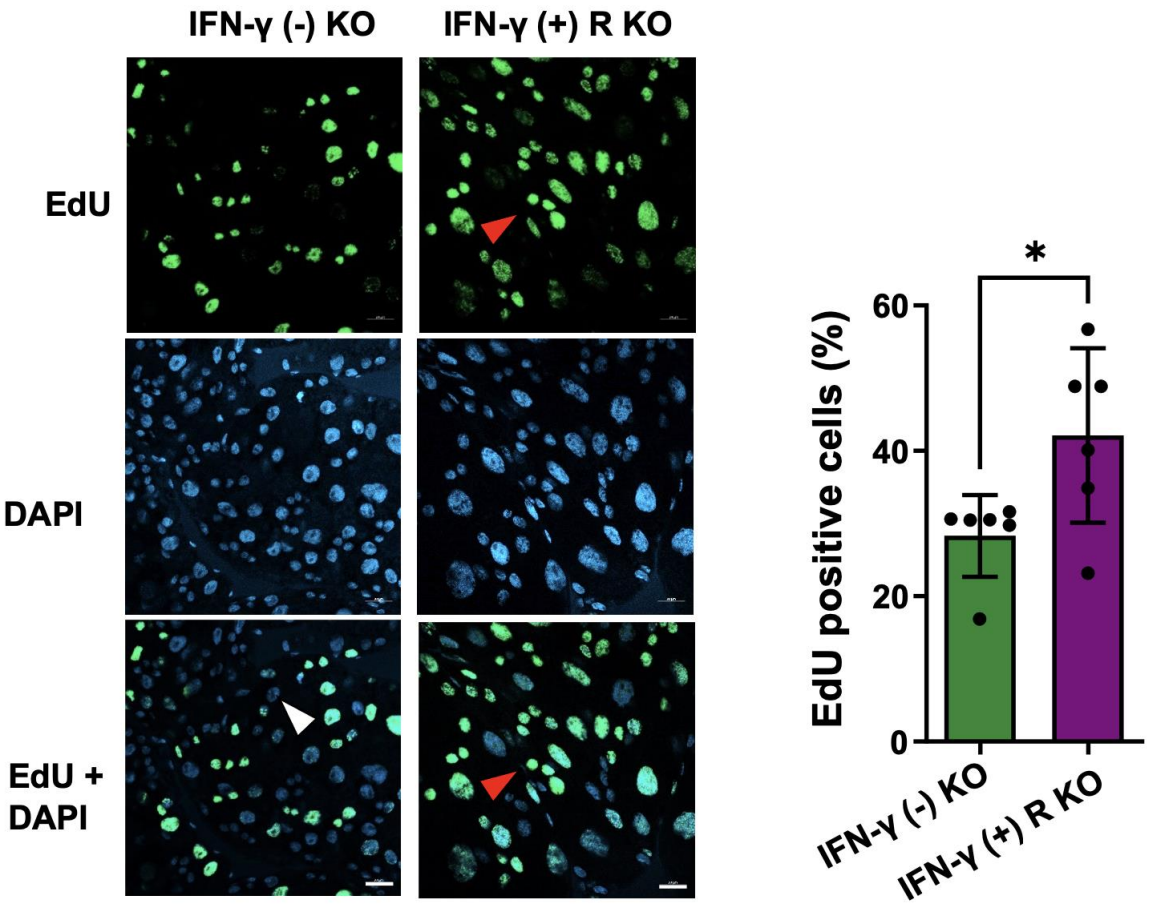

Fig. S14. Host IFN-γ influences cell proliferation in nymphal gut

Groups of IFN-γ-producing or -deficient mice, as described in Fig. 3, were allowed to be parasitized by nymphs for 48 hours, and were then assessed for 5-ethynyl-2′-deoxyuridine (EdU) incorporation, as detailed in Fig. 7. The dissected guts were imaged by confocal microscopy (left panels). A significant reduction in proliferative (EdU positive) cells was observed in ticks that fed on IFN-γ-deficient mice (white arrow), whereas these cells were more abundant in nymphs that fed on IFN-γ-producing mice (red arrow). The tick gut cellular nuclei were labeled with DAPI (blue) or EdU (green). The EdU positive cells from a group of six ticks were enumerated under a confocal microscope (right panel), confirming a significant reduction in proliferative cells in ticks that fed on IFN-γ-deficient mice. Results are representative of two independent experiments. Quantitative data are shown as individual data points and means ± SDs (n = 6). Scale bar = 10 μm, $*P<0.05$, determined using two-tailed Mann–Whitney *U* test.

Fig. S15. Dome1 function in subadult development involves Notch–Delta pathway through *Hox* transcription factors

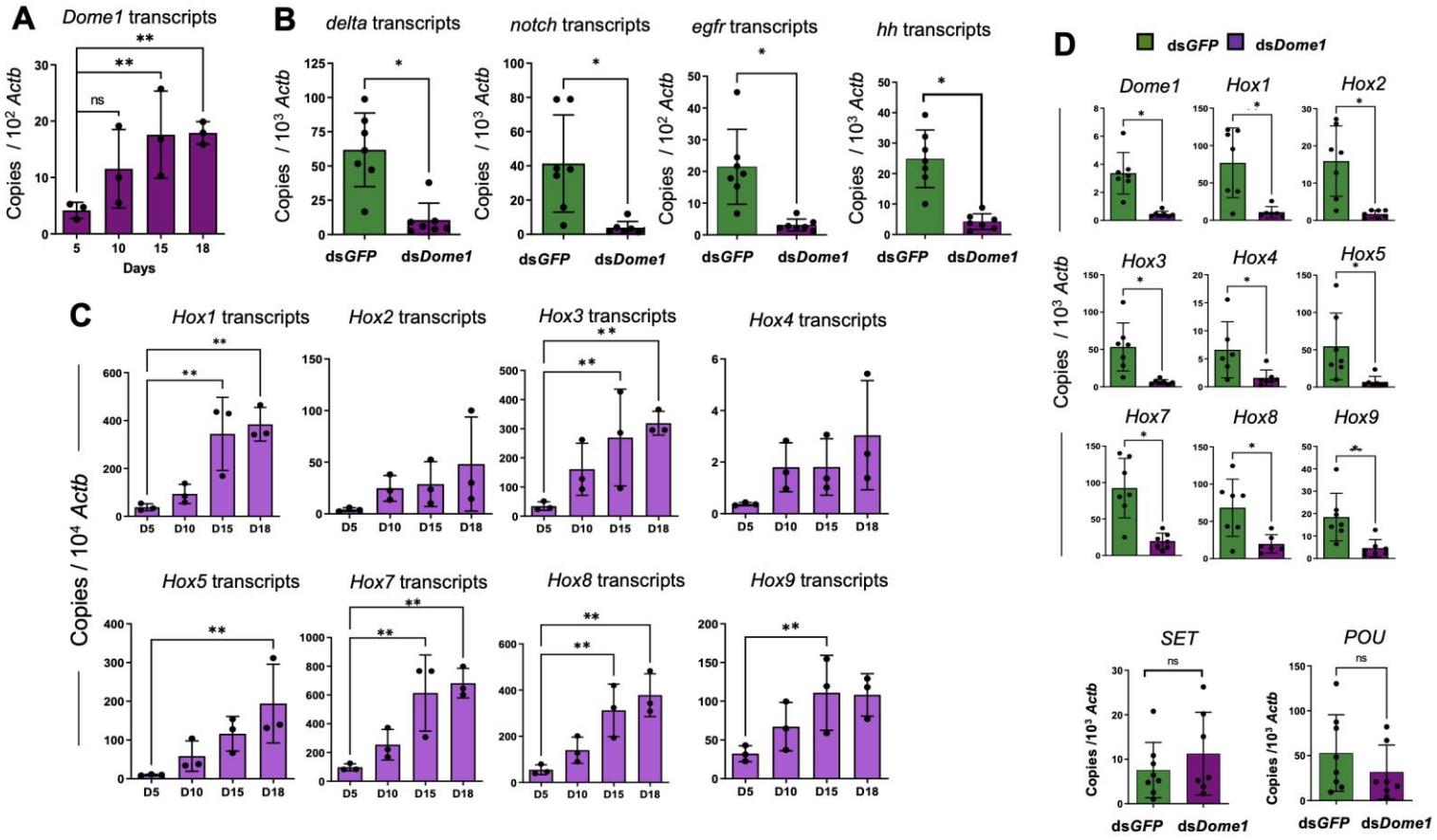

Fig. S15. Dome1 function in subadult development involves Notch–Delta pathway through *Hox* transcription factors

(**A**) Enhanced *Dome1* expression during early larva-to-nymph molting. The relative levels of *Dome1* transcripts in fed larval ticks were analyzed by RT-qPCR at various time points (5, 10, 15, and 18 days after blood meal engorgement). Each dot represents a pool of three larval ticks. ***P*<0.05, determined using one-way ANOVA. (**B**) The knockdown of *Dome1* impairs major transcription factors and signaling pathways related to development. The expression levels of representative target transcripts were analyzed by RT-qPCR during the larva-to-nymph intermolt stage, specifically 15 days after larval blood meal engorgement (8 ticks per group). The transcript levels of *delta*, *notch*, *epidermal growth factor receptor (egfr)*, and *Hedgehog (hh)* were significantly reduced in *Dome1*-knockdown larvae. (**C**) Expression of identified *Hox* genes. The *Hox* genes were analyzed in engorged larval ticks at various time points (5, 10, 15, and 18 days after larval blood meal engorgement) (3 ticks per group). ***P*<0.05, determined using one-way ANOVA. (**D**) The knockdown of *Dome1* impairs the expression of *Hox* genes. The expression levels of the *Hox* genes were analyzed as detailed in panel C. Notably, the expression of all eight *Hox* genes were significantly downregulated in *Dome1*-knockdown ticks, as compared to control (ds*GFP*) ticks, whereas the mRNA levels of the other tested transcription factors, like *SET* or *POU*, remained unaltered (bottom panels). Results are representative of two independent experiments. Quantitative data are shown as individual data points and means ± SDs (n = 3 to 7). **P*<0.05, determined using two-tailed Mann–Whitney *U* test; ns, non-significant.

Fig. S16. RNAi-mediated knockdown of *Hedgehog* yields severe developmental defects in the organs of newly molted nymphs

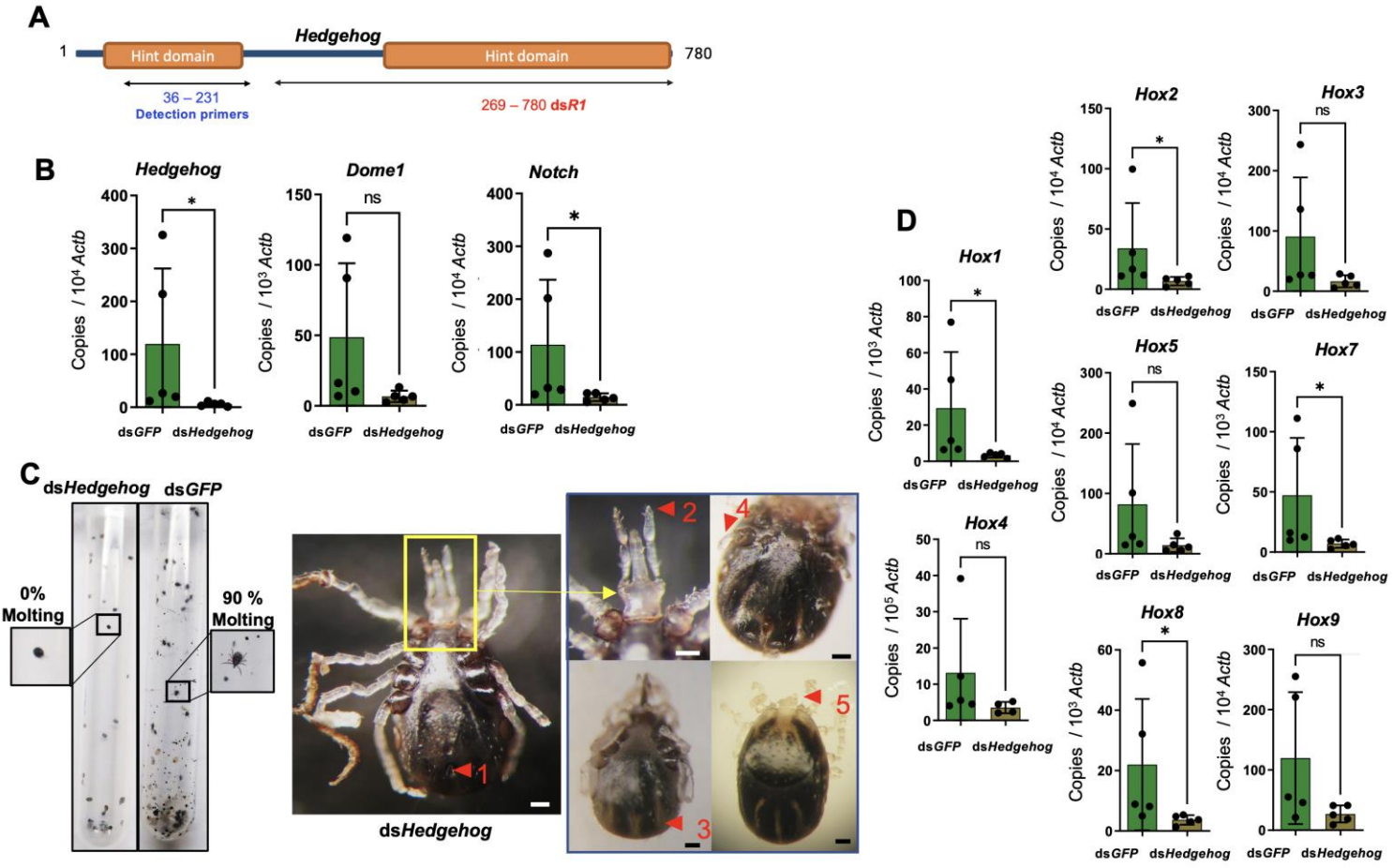

Fig. S16. RNAi-mediated knockdown of *Hedgehog* yields severe developmental defects in the organs of newly molted nymphs

(**A**) Schematic representation of the *Hedgehog* open reading frame showing regions targeted for RNAi. The regions encompassing the dsRNA construct (ds*R1*, red) and detection primers (blue) are shown. (**B**) The knockdown of *Hedgehog* in larval ticks. Groups of fed larvae (25 ticks per group) were microinjected either with ds*Hedgehog* or control ds*GFP* RNA (4 µg/µl) and then fed on *B. burgdorferi*-infected mice. The intermolt ticks were then processed for RT-qPCR assessment of mRNA levels using gene-specific primers, normalizing against tick *Actb* levels. (**C**) *Hedgehog*-knockdown ticks were unable to molt. The fed knockdown larvae, as detailed in panel B, were allowed to molt, and were then analyzed as newly molted unfed nymphs. None of the *Hedgehog*-knockdown ticks were able to molt, whereas 90% of the control (ds*GFP*) ticks successfully molted to nymphs. The right panels show intermolt *Hedgehog*-knockdown ticks displaying deformities, such as a defective anal pore (1), malformed mouthparts (2), darker abdomen (3), abnormal legs (4), and sometimes the complete loss of mouthparts (5). These developmental defects are comparable to *Dome1*-, *JAK*-, or *STAT*-knockdown ticks (Fig. 4, fig. S10, and fig. S12). Scale bar (black or white) = 50 µm. (**D**) The knockdown of *Hedgehog* impairs several *Hox* transcription factors related to the *Hedgehog* signaling pathway for development. The expression of target transcripts were analyzed by RT-qPCR during the larva-to-nymph intermolt stage, specifically 15 days after larval blood meal engorgement (8 ticks per group). The transcript levels of *Hox1*, *Hox2*, *Hox7*, and *Hox8* were significantly reduced in *Hedgehog*-knockdown larvae. Results are representative of two independent experiments. Quantitative data are shown as individual data points and means ± SDs (n = 5 to 50). **P*<0.05, determined using two-tailed Mann–Whitney *U* test; ns, non-significant.

Fig. S17. Conservation of Dome1–JAK–STAT signaling components across genomes of major tick vectors

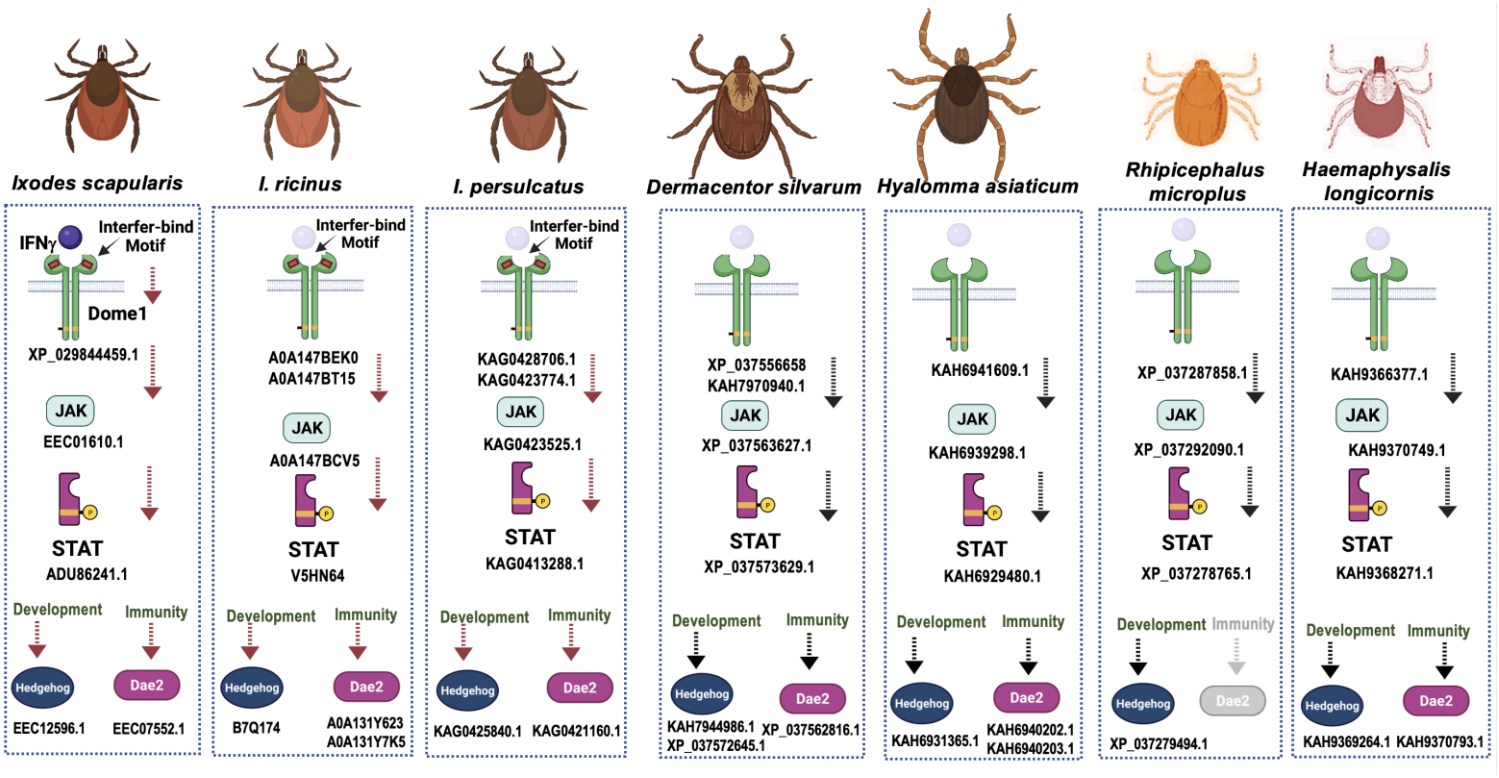

Fig. S17. Conservation of Dome1–JAK–STAT signaling components across genomes of major tick vectors

Orthologs of Dome1 and associated representative signaling components relevant to arthropod development and immunity, such as JAK, STAT, Hedgehog, and Dae2, were searched across major databases. Their presence in these databases, including their accession numbers, are indicated by colored diagrams. Except for the apparent absence of Dae2 (gray image) in *Rhipicephalus microplus*, these signaling components are identifiable in all major tick species. The interfer-bind motif that binds IFN-γ is mostly conserved in all examined *Ixodes* spp. ticks.

Fig. S18. Primary sequence alignment of Dome1 orthologs in representative tick species

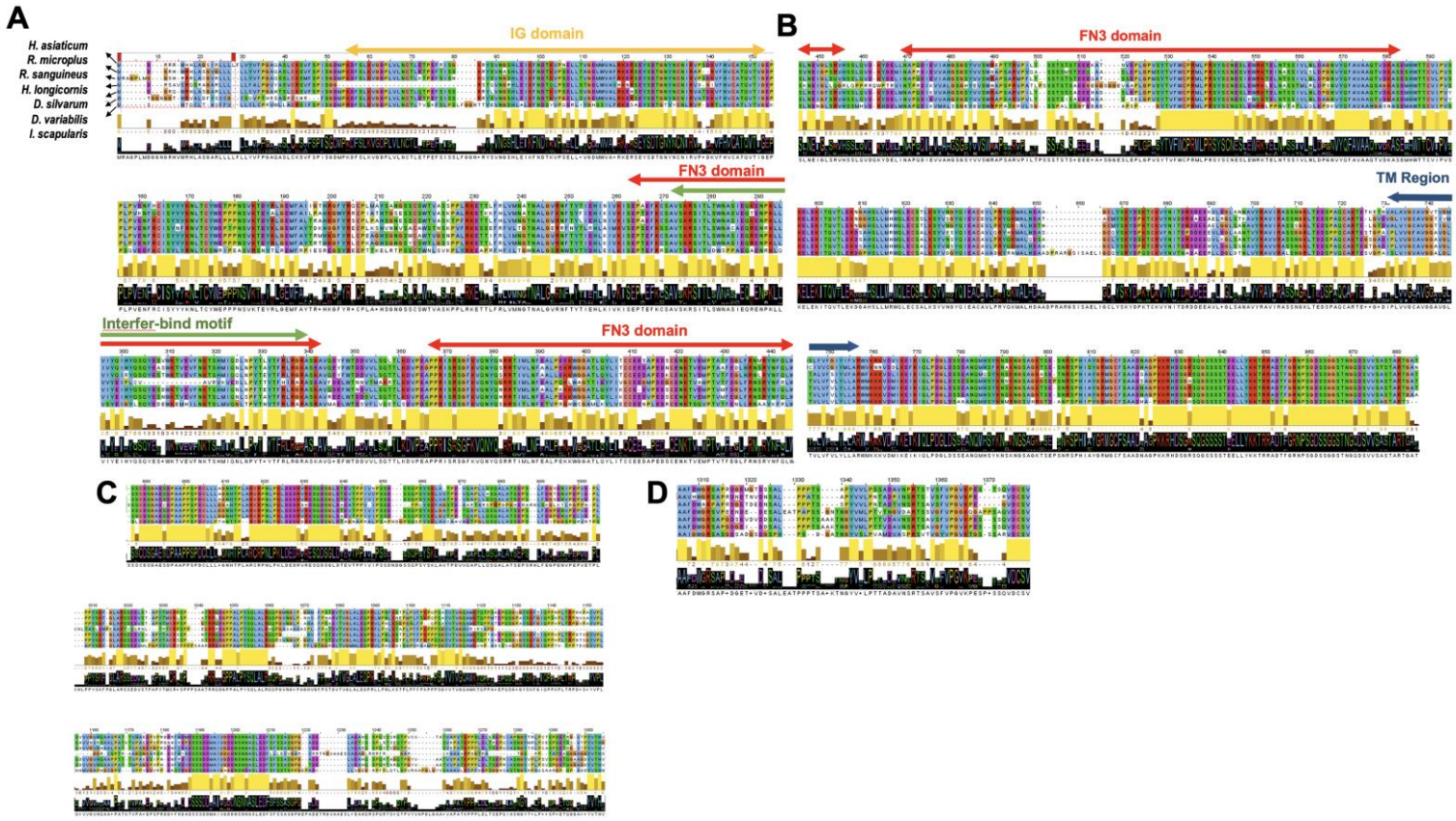

Fig. S18. Primary sequence alignment of Dome1 orthologs in representative tick species

The amino acid sequence homology between Dome homologs from *Ixodes scapularis* and the following other tick species are indicated: *Hyalomma asiaticum*, *Rhipicephalus microplus*, *R. sanguineus*, *Haemaphysalis longicornis*, *Dermacentor silvarum*, and *D. variabilis*. Amino acids with similar properties are labeled with identical colors. The locations of the identifiable domains, including the IG domain, interfer-bind motif, three fibronectin type-III (FN3) domains, transmembrane (TM) domain, and the rest of the cytoplasmic regions are shown. The panels A-D represent the sequential sequence alignments, starting from the amino termini through the carboxyl termini of these sequences, as detailed in the Materials and Methods section.

Fig. S19. Dome1 orthologs are expressed in non-*Ixodes* ticks during tick engorgement on hosts

Fig. S19. Dome1 orthologs are expressed in non-*Ixodes* ticks during tick engorgement on hosts

Temporal expression of *Dome1* ortholog in the American dog tick, *D. variabilis* (left panel), and the lone star tick, *A. americanum* (right panel). Nymphs were allowed to parasitize guinea pigs, and partially fed ticks were then collected at various time points during feeding between day 1 to day 4. *Dome* transcript levels were analyzed by RT-qPCR. An independent experiment is shown (n = 7 to 50).

Fig. S20. *Dome1* ortholog in *D. variabilis* supports tick gut cellular proliferation and microbial homeostasis

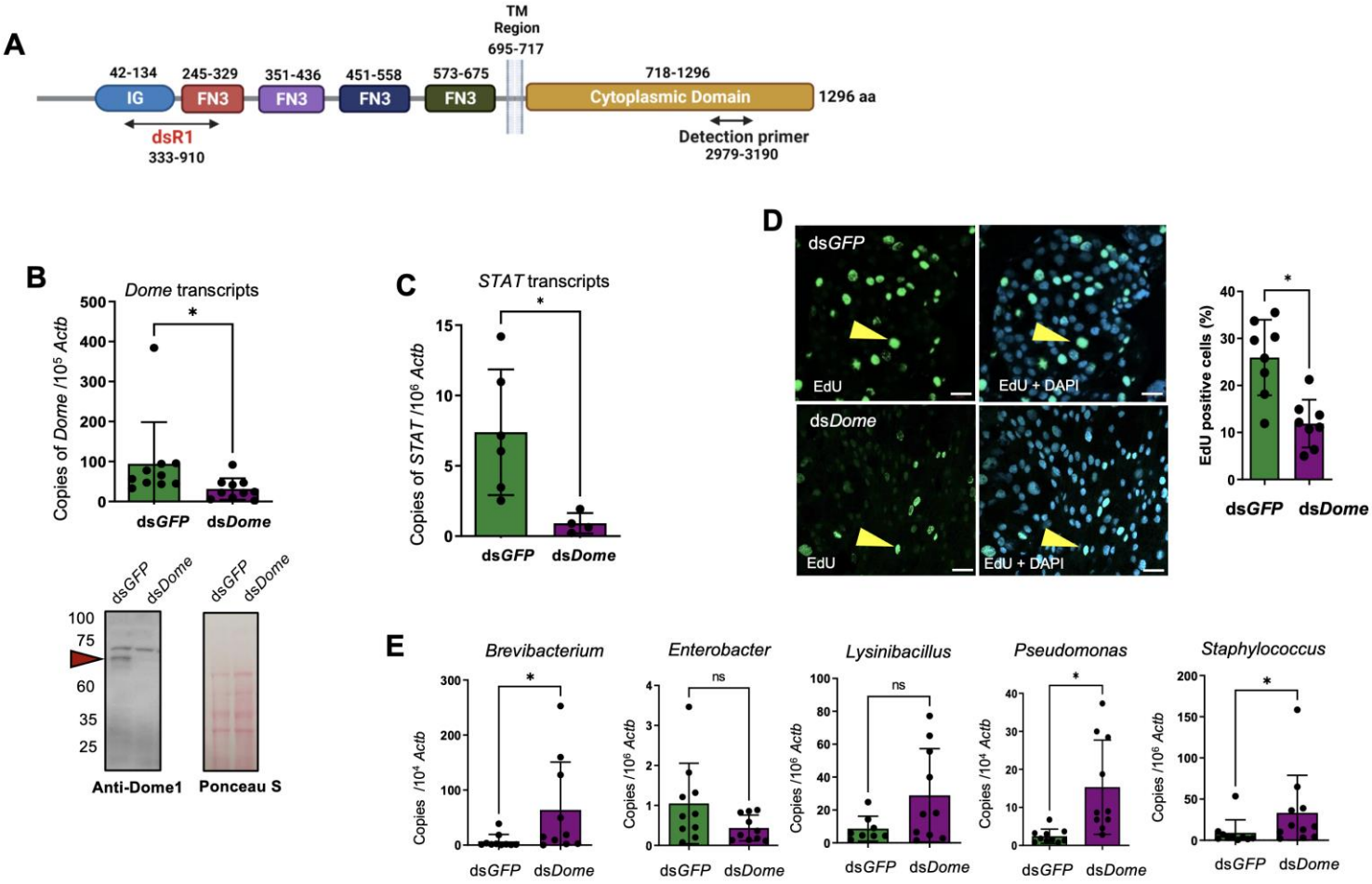

Fig. S20. *Dome1* ortholog in *D. variabilis* supports tick gut cellular proliferation and microbial homeostasis

(**A**) Schematic diagram showing features of *Dome1* ortholog in *D. variabilis*, designated as *Dome*. The domains (IG, four fibronectin type-III [FN3], transmembrane [TM], and cytoplasmic) with amino acid (aa) positions indicated. The regions (including nucleotide positions) for RNAi (ds*R1*) as well as detection primers used for the assessment of transcript silencing via RT-qPCR analysis are shown. (**B**) The knockdown of *Dome* in *D. variabilis* nymphs. Ticks (30 per group) were microinjected with ds*Dome* or control ds*GFP* RNA (4 µg/µl) and then fed on guinea pigs for 72 hours. The partially fed ticks were processed for *Dome* mRNA levels using specific primers and normalizing against tick *Actb* levels (upper panel). The level of Dome protein in *D. variabilis* was analyzed by western blotting using polyclonal antibodies generated against *I. scapularis* Dome1 (lower panel). The arrow denotes the Dome ortholog in *D. variabilis.* (**C**) Knockdown of *Dome* in *D. variabilis* downregulates *STAT* expression. The partially fed ticks were processed for mRNA levels using specific primers and normalizing against tick *Actb* levels. (**D**) Cell proliferation in the nymphal *D. variabilis* gut. Nymphal ticks fed on guinea pigs for 72 hours to initiate gut cell proliferation. Next, nymphs were collected, microinjected with EdU (green), and allowed to rest while the fluorescent nucleoside analog was incorporated into tick DNA. The tick guts were then dissected and imaged by confocal microscopy. Proliferative EdU positive cells are shown by arrows. The EdU positive cells from a group of seven ticks were enumerated under a confocal microscope (right panel), confirming a severe reduction in proliferative cells in *Dome*-knockdown ticks. The tick nuclei were labeled using DAPI (blue). Scale bar = 20 µm. (**E**) *Dome* knockdown imparts alterations in microbial homeostasis in the *D. variabilis* gut. Ticks were allowed to partially

engorge on guinea pigs. Dissected guts from individual nymphs were analyzed via RT-qPCR targeting 16S rRNA transcripts from representative microbial species. Results are representative of two independent experiments. Quantitative data are shown as individual data points and means ± SDs (n = 6 to 9). *P<0.05, determined using two-tailed Mann–Whitney U test; ns, non-significant.

Fig. S21. Alternate dsRNA strategy for independent *Dome1* knockdown did not alter other *Dome* homologs, yet imparted similar phenotypic defects observed for primary dsRNA constructs

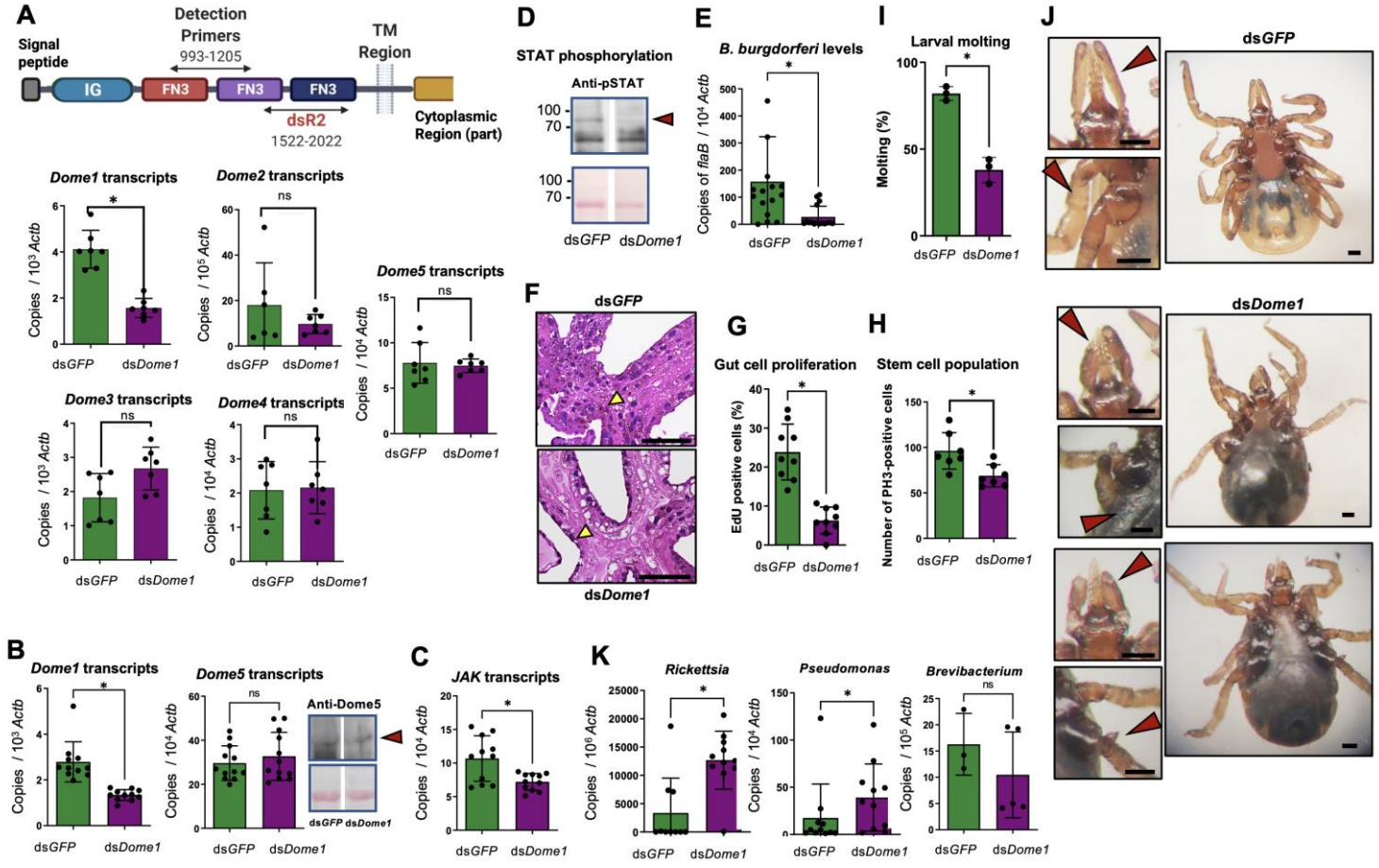

Fig. S21. Alternate dsRNA strategy for independent *Dome1* knockdown did not alter other *Dome* homologs, yet imparted similar phenotypic defects observed for primary dsRNA constructs

(**A**) Schematic representation of the *Dome1* open reading frame, showing regions targeted for RNAi (upper panel), including the alternate dsRNA construct (ds*R2*). The lower panels denote the selective knockdown of *Dome1* irrespective of any impact on other *Dome* homologs. (**B**) *Dome1* knockdown did not influence expression of *Dome5* mRNA or protein (arrow) levels. (**C**) *Dome1* knockdown impairs *JAK* expression, as shown by RT-qPCR. (**D**) *Dome1* knockdown reflects decreased levels of phosphorylated STAT (arrow), as shown by immunoblotting (upper panel). Equal protein loading was evidenced by Ponceau S staining (lower panel). (**E**) Knockdown of *Dome1* impairs *B. burgdorferi* levels within the tick gut, as examined via measuring *flaB* transcripts and normalizing to tick *Actb* using RT-qPCR. (**F to H**) *Dome1* knockdown reduces the proliferation of gut cells, as revealed by histological analysis (panel F), incorporation of EdU (panel G), and assessment of gut stem cells (panel H), using methods detailed in Fig. 7. Scale bar = 100 µm. (**I**) *Dome1* knockdown affects larva-to-nymph molting. Fed knockdown larvae, as detailed in panel A, were allowed to molt and then enumerated. (**J**) *Dome1* knockdown influences proper development of nymphs, as imaged under a dissecting binocular microscope, showing severe phenotypic deformities, including abnormal hypostomes and legs (red arrowheads). Scale bar = 50 µm. (**K**) *Dome1* knockdown alters tick gut microbiota. Ticks partially engorged on *B. burgdorferi*-infected mice and gut samples were analyzed via RT-qPCR using 16S rRNA targeting selected bacterial genera. Results are representative of two to three independent experiments. Quantitative data are shown as individual data points and means ± SDs (n = 7 to 50) *P<0.05, determined using two-tailed Mann–Whitney *U* test; ns, non-significant.

Table S1: **Differentially produced proteins between *B. burgdorferi*-infected and naïve controls (both tick groups injected with ds*GFP*)**

Accession number	Description	Abundance Ratio (%): (Infected ds*GFP*) / (Naïve ds*GFP*)
A0A4D5RRR3	Tetraspanin	7.261
M4PN64	Cytochrome c oxidase subunit 1 (Fragment)	5.992
A0A4D5SB93	Putative low-density lipoprotein receptor (Fragment)	2.902
A0A4D5RHI9	Putative epithelial chloride channel protein	2.27
A0A4D5RU19	Putative nucleolar and coiled-body phosphoprotein 1 (Fragment)	2.261
B7P3D1	Tpr and ank domain-containing protein, putative	2.229
A0A4D5RZX3	Putative dehydrogenase (Fragment)	2.136
A0A4D5S3U1	Putative molecular chaperone distantly (Fragment)	2.072
B7QKR4	25 kDa salivary gland protein C, putative	2.059
B7PJA0	Secreted protein, putative	2.042
A0A4D5RQP0	Putative conserved secreted protein (Fragment)	2.011
A0A4D5RQS3	SF3 helicase domain-containing protein (Fragment)	1.986
A0A4D5S5L7	Putative acyl-coa synthetase (Fragment)	1.866
B7P3V7	Uncharacterized protein	1.765
B7PFF0	Secreted protein, putative	1.748
B7PPE2	Tnf receptor associated factor, putative (Fragment)	1.733
B7Q203	ATPase, putative	1.729
B7P3N0	Protein disulfide isomerase 3, putative (Fragment)	1.718
A0A4D5RV46	Putative cytochrome p450 cyp3/cyp5/cyp6/cyp9 subfamily protein	1.707
A0A4D5S320	Putative nicotinamide n-methyltransferase (Fragment)	1.701
A0A4D5RAF8	Putative presenilins-associated rhomboid-like protein (Fragment)	1.683
A0A4D5RY03	Putative tick transposon (Fragment)	1.645
A0A4D5RQ02	Uncharacterized protein (Fragment)	1.638
B7Q2B6	Secreted salivary gland peptide, putative	1.636
A0A4D5RVD6	Putative lipoprotein amino terminal region	1.62
B7QHR8	Zinc/iron transporter, putative	1.611
B7QBB4	Uncharacterized protein	1.604

B7QNY6	Serine proteinase inhibitor serpin-3, putative	1.593
A0A4D5RUL4	Putative serine proteinase inhibitor	1.591
A0A4D5RBQ9	Ig-like domain-containing protein	1.588
B7PSV2	Methyltransf_11 domain-containing protein	1.585
B7QM70	Small heat shock protein, putative (Fragment)	1.577
B7QNV8	Uncharacterized protein	1.574
A0A4D5S0E2	Phospholipase B-like (Fragment)	1.567
B7Q013	L-allo-threonine aldolase, putative	1.557
B7PFB3	N-methyltransferase, putative (Fragment)	1.557
A0A4D5RBE8	Uncharacterized protein (Fragment)	1.552
B7PPM4	Histone-lysine N-methyltransferase, setb1, putative	1.549
A0A4D5RNU3	BTB domain-containing protein (Fragment)	1.545
B7QH07	Cytoplasmic dynein heavy chain, putative	1.541
Q95WZ5	Histamine binding protein	1.54
A0A4D5RS29	Putative atp-dependent rna helicase (Fragment)	1.532
A0A4D5RMJ7	Putative tick serine proteinase (Fragment)	1.527
B7PNH7	Uncharacterized protein	1.523
A0A4D5RM16	Putative conserved secreted protein (Fragment)	1.515
A0A4D5REH9	Putative lipid phosphate phosphatase	1.515
B7PMF3	Secreted protein, putative	1.505
B7Q1W5	Elongation factor 1 gamma, putative	0.66
B7PS13	ING (mammalian INhibitor of Growth) family protein (ing3)-like, putative (Fragment)	0.66
B7PCZ5	Glutathione synthetase, putative (Fragment)	0.658
A0A4D5RRW2	Putative transporter (Fragment)	0.649
A0A4D5RST0	Putative acyl-coa synthetase (Fragment)	0.638
Q8MVB0	Truncated secreted metalloprotease	0.624
B7PLJ6	Glycerol-3-phosphate dehydrogenase [NAD(+)]	0.621
A0A088CQT2	Cytochrome c oxidase subunit 1 (Fragment)	0.617
B7PAY9	Calbindin-32, putative	0.61
A0A4D5RLE2	Putative fructose-16-bisphosphatase (Fragment)	0.603
B7P7W6	Innexin	0.602
B7PJW6	Chitin deacetylase 9, putative	0.594
B7P1H9	Neurotrimin, putative (Fragment)	0.592
A0A4D5RQN5	Putative secreted protein (Fragment)	0.568
B7Q265	Sphingomyelin phosphodiesterase, putative (	0.565

A0A4D5RJ63	Putative muscle m-line assembly protein unc-89	0.564
B7Q1Z5	Uncharacterized protein	0.559
A0A1S4KT52	WD-repeat protein, putative	0.554
A0A4D5RD42	Putative eukaryotic translation initiation factor 4 gamma 1-like isoform x2 (Fragment)	0.529
Q4PMP3	Putative secreted salivary protein	0.501
A0A4D5S981	CRAL_TRIO_N domain-containing protein (Fragment)	0.476
A0A4D5RT62	Putative glutathione s-transferase (Fragment)	0.449
A0A4D5RU61	Putative hydroxysteroid 17-beta dehydrogenase 11 (Fragment)	0.225

Table S2: **Differentially produced proteins between *Dome1*-knockdown and control (ds*GFP*-injected) ticks**

Accession number	Description	Abundance Ratio (%): (ds*Dome1*) / (ds*GFP*)
A0A4D5RRR3	Tetraspanin	6.719
M4PN64	Cytochrome c oxidase subunit 1 (Fragment)	6.51
B7QKR4	25 kDa salivary gland protein C, putative	5.772
A0A4D5SB93	Putative low-density lipoprotein receptor (Fragment)	5.292
A0A4D5RK09	Putative regulation of transcription (Fragment)	5.149
B7Q8I4	CABIT domain-containing protein	5.056
A0A4D5S4Q9	Putative salivary secreted protein with polyk tail	4.643
Q5S1X6	Fed tick salivary protein 4	4.14
B7P3G0	Chitinase, putative (Fragment)	3.877
B7Q2C1	Metalloprotease, putative	3.839
Q8MVB0	Truncated secreted metalloprotease	3.452
A0A4D5REU5	Putative pancreatic lipase-like enzyme (Fragment)	3.439
B7P1H9	Neurotrimin, putative (Fragment)	3.217
B7Q0V7	Secreted protein, putative (Fragment)	3.166
B7PCM5	Uncharacterized protein	3.164
F6KSY1	Salivary protein antigen P8	3.021
B7PQF4	Sulfotransferase, putative	3.006
A0A1S4M4I5	Salivary gland metalloprotease, putative	2.949
B7PUC0	AKAP2_C domain-containing protein	2.909
B7PYE3	Secreted salivary gland peptide, putative (Fragment)	2.896
Q95WZ5	Histamine binding protein	2.894
B7QFI5	Cell adhesion molecule, putative	2.795
B7QM92	Peptidase M12B domain-containing protein	2.787
B7PLN8	Secreted protein, putative	2.729
Q8MVB9	Uncharacterized protein	2.685
A0A4D5RAJ8	Putative secreted metalloprotease	2.682
B7Q2B8	Metalloprotease, putative	2.666
B7QFF3	Lipase, putative (Fragment)	2.645
B7PJA0	Secreted protein, putative	2.547
B7PPM4	Histone-lysine N-methyltransferase, setb1, putative	2.47
A0A4D5RG89	Putative focal adhesion adaptor protein paxillin (Fragment)	2.469
B7P635	Sulfotransferase, putative	2.467
B7PTV6	FYVE-type domain-containing protein (Fragment)	2.456
A0A4D5S5P0	Uncharacterized protein	2.406
B7PMM0	Uncharacterized protein	2.404

Q4PMX1	Putative salivary HBP family member	2.404
B7QNS1	Amino acid transporter	2.355
A0A4D5RLP0	Putative cholesterol transport protein	2.336
A0A4D5RN87	Putative serine proteinase inhibitor	2.32
A0A4D5RLH3	Putative pancreatic lipase-like enzyme (Fragment)	2.244
A0A4D5S4C3	Uncharacterized protein (Fragment)	2.214
B7P1H7	Titin, putative	2.209
B7Q2X5	Phosphoinositol 4-phosphate adaptor protein, putative	2.203
Q8MVG3	Putative secreted protein	2.198
A0A4D5RXM4	Calreticulin	2.183
A0A4D5RM16	Putative conserved secreted protein (Fragment)	2.16
Q4PNA3	Putative secreted protein with basic tail	2.141
A0A4D5RDR9	Putative vacuolar assembly/sorting (Fragment)	2.127
A0A4D5RQI3	Putative salivary secreted peptide	2.113
Q4PML3	Putative salivary secreted protein	2.106
A0A4D5RX10	Protein disulfide-isomerase	2.105
B7PMM4	ABC transporter, putative (Fragment)	2.104
A0A4D5RR07	Putative conserved secreted protein	2.103
B7Q4J7	Glutathione S-transferase, putative	2.097
A0A4D5RGT9	Putative secreted protein (Fragment)	2.066
A0A4D5RQY6	Putative pdz domain-containing protein (Fragment)	2.062
A0A4D5RMT9	Putative cholesterol transport protein	2.059
B7QK00	Uncharacterized protein (Fragment)	2.047
A0A4D5RT05	Putative s phase cyclin a-associated protein in the endoplasmic reticulum (Fragment)	2.045
A0A4D5RZ46	Putative non-muscle myosin heavy chain ii	2.035
A0A1S4M122	Actin, putative	2.03
B7PV21	Synaptotagmin-14, putative	2.003
A0A4D5RJY2	Putative hemolectin (Fragment)	2.002
B7PPE2	Tnf receptor associated factor, putative (Fragment)	1.998
B7PTN7	Prolyl 4-hydroxylase alpha subunit, putative (Fragment)	1.992
B7Q4N7	Uncharacterized protein	1.963
B7PIV2	Uncharacterized protein	1.948
A0A4D5RGQ6	Putative serine proteinase inhibitor	1.945
B7Q1H6	Laminin gamma-1 chain, putative (Fragment)	1.942
A0A4D5RQM6	Putative hyaluronan mediated motility receptor (Fragment)	1.929
B7QCM5	Ribose-5-phosphate isomerase, putative (Fragment)	1.923
B7P2U1	Uncharacterized protein	1.917
B7P3N0	Protein disulfide isomerase 3, putative (Fragment)	1.902
B7Q713	Astacin, putative	1.898

B7PMF3	Secreted protein, putative	1.897
A0A4D5RQ02	Uncharacterized protein (Fragment)	1.887
A0A4D5REN9	Putative guanine nucleotide binding protein mip1	1.886
B7P1I0	Titin, putative	1.875
A0A4D5RIY3	Methionine aminopeptidase (Fragment)	1.865
A0A4D5RKW6	Putative l-threonine 3-dehydrogenase mitochondrial-like protein (Fragment)	1.861
A0A4D5RGG2	Putative guanylate-binding protein (Fragment)	1.851
A0A4D5RRX9	Putative ml domain protein	1.846
B7PL51	ML domain-containing protein, putative	1.845
B7QMM1	Glycine C-acetyltransferase/2-amino-3-ketobutyrate-CoA ligase, putative (Fragment)	1.832
B7PZH4	Animal-type fatty acid synthase, putative	1.831
B7P1I1	Secreted protein, putative (Fragment)	1.831
B7P5L3	Nymphal histamine binding protein B, putative (Fragment)	1.824
A0A4D5RY03	Putative tick transposon (Fragment)	1.808
A0A4D5RNY4	Glucosylceramidase	1.796
B7PS64	Cytochrome P450, putative (Fragment)	1.793
B7QKG0	ACB domain-containing protein	1.791
A0A4D5S3C6	Putative tp53-induced glycolysis and apoptosis regulator b (Fragment)	1.783
A0A4D5RGX3	Putative tick serine proteinase (Fragment)	1.774
A0A4D5RC42	Putative elongation factor-1 gamma (Fragment)	1.772
B7P9L7	Preprodefensin, putative	1.772
B7PAY4	Zinc phosphodiesterase, putative	1.766
A0A4D5RVG6	Putative sulfotransferase	1.765
A0A4D5RFD8	Putative serine protease	1.761
B7PG23	Serine proteinase inhibitor, putative	1.758
B7PH23	Secreted protein, putative	1.75
B7QJ79	Replication factor C, subunit RFC2, putative	1.749
B7Q032	Uncharacterized protein	1.746
A0A4D5RPH6	Putative copper-transporting atpase 1	1.744
B7P101	Membrane glycoprotein LIG-1, putative	1.741
A0A4D5S4H2	Putative acetylcholinesterase/butyrylcholinesterase (Fragment)	1.733
B7PQ22	Crystal protein, putative	1.729
B7Q2B6	Secreted salivary gland peptide, putative	1.723
B7Q9D9	RAB GTPase-activating protein, putative (Fragment)	1.722
A0A4D5RQD8	Putative programmed cell death protein (Fragment)	1.722
A0A4D5RQW5	Putative membrane glycoprotein lig-1	1.721
A0A4D5RFZ2	Putative serine proteinase inhibitor	1.72
A0A4D5RK10	Putative membrane glycoprotein lig-1	1.717

A0A4D5S320	Putative nicotinamide n-methyltransferase (Fragment)	1.716
A0A4D5RG78	Putative adp-ribosylglycohydrolase posttranslational modification (Fragment)	1.71
A0A4D5RFM0	Putative serine protease (Fragment)	1.708
B7P1J7	Uncharacterized protein	1.697
A0A4D5S7Q5	Putative cystatin iscys1	1.696
A0A4D5RRJ5	Glutathione peroxidase (Fragment)	1.69
A0A4D5S4S9	Uncharacterized protein (Fragment)	1.686
B7QGM6	Phospholipase A2 precursor, putative	1.686
A0A4D5RLH7	Putative 4-hydroxyphenylpyruvate dioxygenase (Fragment)	1.682
A0A1S6Y024	Reeler domain-containing gut protein	1.68
B7P3D1	Tpr and ank domain-containing protein, putative	1.679
B7P102	Membrane glycoprotein lig1, putative	1.671
A0A4D5S597	Putative n6-adenine-specific dna methyltransferase (Fragment)	1.668
A0A4D5RHN9	Putative fanconi anemia group i protein	1.665
A0A4D5RMD2	Putative conserved secreted protein	1.663
B7PA38	Peptidyl-prolyl cis-trans isomerase E	1.662
B7PUF8	Adenylate cyclase, putative (Fragment)	1.661
A0A4D5RNU3	BTB domain-containing protein (Fragment)	1.657
B7Q013	L-allo-threonine aldolase, putative	1.657
A0A4D5S5Z5	Putative conserved secreted protein	1.653
A0A4D5RXW7	Putative ezrin/radixin/moesin family (Fragment)	1.648
B7P2I1	Oxysterol-binding protein (Fragment)	1.647
A0A4D5S337	Putative antimicrobial peptide	1.646
A0A4D5REA9	Glucose-6-phosphate isomerase	1.641
B7PSK7	Alanine-glyoxylate aminotransferase, putative	1.625
B7Q9Y6	Rif1_N domain-containing protein	1.618
A0A4D5RJD5	Putative notch signaling protein (Fragment)	1.611
A0A4D5S4X0	Putative epithelin/granulin (Fragment)	1.611
A0A4D5RKR3	Putative cytochrome (Fragment)	1.611
A0A4D5RHM2	Putative positive regulation of cytokine secretion (Fragment)	1.61
A0A4D5S093	Putative vegetative cell wall protein gp1 (Fragment)	1.606
A0A4D5RVD6	Putative lipoprotein amino terminal region	1.603
B7QL39	Translation elongation factor G, putative (Fragment)	1.601
A0A4D5S7C6	Putative antimicrobial peptide	1.597
A0A4D5RST4	Carboxylic ester hydrolase (Fragment)	1.596
A0A4D5RTN0	Putative membrane protein	1.595
B7PW73	Transcription initiation factor TFIID subunit 10	1.592
A0A4D5RPJ9	Uncharacterized protein (Fragment)	1.591
A0A4D5RZZ4	Putative enteropeptidase isoform x2	1.582

B7P7W6	Innexin	1.573
A0A4D5S634	Uncharacterized protein (Fragment)	1.569
A0A4D5RB00	Putative macrophage migration inhibitory factor (Fragment)	1.566
A0A4D5S624	Putative serine proteinase (Fragment)	1.565
A0A4D5RL41	Putative sodium-bile acid cotransporter	1.564
A0A4D5SB43	Putative cathepsin b endopeptidase	1.564
B7PLF9	Kinesin-associated protein, putative	1.561
B7PR02	Peptidase_M28 domain-containing protein	1.56
B7PYL3	Dehydrogenase, putative	1.557
A0A4D5RS25	Putative rna polymerase-associated protein ctr9 (Fragment)	1.555
B7PK57	Uncharacterized protein	1.554
B7PBF8	ADP ribosylation factor 79F, putative (Fragment)	1.55
A0A4D5RLI9	Putative p450 (Fragment)	1.55
B7QNH1	Triacylglycerol lipase, putative (Fragment)	1.549
A0A4D5RFT9	Putative elongation factor 2 (Fragment)	1.547
B7P8V8	Uncharacterized protein	1.546
A0A4D5RFC8	Putative histone acetyltransferase saga trrap/tra1 component pi-3 kinase superfamily protein (Fragment)	1.545
B7Q4V8	Uncharacterized protein	1.543
B7PGR7	Uncharacterized protein	1.542
B7Q0L0	Uncharacterized protein	1.542
B7QKR7	Secreted protein, putative	1.54
B7P8S8	Gar2, putative	1.537
B7PHX3	Chymotrypsin-C precursor, putative	1.536
A0A4D5RRL1	Putative asparaginyl peptidase (Fragment)	1.535
A0A4D5RUJ6	Putative secreted protein (Fragment)	1.535
A0A4D5RQF0	Putative aquaporin (Fragment)	1.532
B7PR40	SCP domain-containing protein	1.528
A0A4D5RG65	Putative membrane glycoprotein lig-1	1.527
B7QIK8	Chitinase, putative	1.525
A0A4D5RUK8	Putative snf2 family dna-dependent atpase (Fragment)	1.524
A0A4D5RYS5	Putative peritrophic membrane chitin binding protein (Fragment)	1.521
A0A4D5RJV0	Putative transcription factor (Fragment)	1.52
A0A4D5RJW4	Putative phd finger protein (Fragment)	1.519
B7PXA4	Ves G 1 allergen precursor, putative (Fragment)	1.518
A0A4D5RIG3	Putative cytochrome	1.518
A0A4D5S0E2	Phospholipase B-like (Fragment)	1.51
B7P370	Ferrochelatase	1.51
A0A4D5SAY3	Putative fatty acid synthase (Fragment)	1.51

B7QI18	RAB GDP/GTP exchange factor, putative	1.503
A0A4D5RWD4	Putative tir domain protein (Fragment)	1.502
B7Q911	tRNA pseudouridine synthase	1.499
B7Q0I5	Proteasome, subunit beta, putative	0.665
B7QL12	Glycyl-tRNA synthetase, putative	0.663
A0A4D5RU61	Putative hydroxysteroid 17-beta dehydrogenase 11 (Fragment)	0.656
B7P5P9	Cuticle protein, putative	0.647
A0A4D5RPD2	Dolichyl-diphosphooligosaccharide--protein glycosyltransferase subunit 2 (Fragment)	0.638
B7PB63	Leucine-rich transmembrane protein, putative	0.624
A0A4D5RUL4	Putative serine proteinase inhibitor	0.606
B7PPR2	Cytochrome P450, putative	0.588
A0A4D5RLE2	Putative fructose-16-bisphosphatase (Fragment)	0.567
B7P6X9	Hemolectin, putative (Fragment)	0.559
B7PQQ9	Selenium-binding protein, putative (Fragment)	0.541
A0A4D5RPX9	Putative o-methyltransferase (Fragment)	0.524
A0A4D5RVM4	Putative multiple coagulation factor deficiency 2-like protein (Fragment)	0.43
A0A1S4KT52	WD-repeat protein, putative	0.351
A0A4D5RS70	Putative sulfotransferase (Fragment)	0.351

Table S3: **Differentially produced proteins between *B. burgdorferi*-infected *Dome1*-knockdown and *B. burgdorferi*-infected control (ds*GFP*-injected) ticks**

Accession number	Description	Abundance Ratio (%): (Infected ds*Dome1*) / (Infected ds*GFP*)
A0A4D5SB93	Putative low-density lipoprotein receptor (Fragment)	2.192
B7Q6J1	GGY domain-containing protein, putative (Fragment)	1.809
A0A4D5RK09	Putative regulation of transcription (Fragment)	1.799
A0A4D5RG89	Putative focal adhesion adaptor protein paxillin (Fragment)	1.782
A0A4D5S4S9	Uncharacterized protein (Fragment)	1.767
M4PN64	Cytochrome c oxidase subunit 1 (Fragment)	1.754
A0A4D5RT05	Putative s phase cyclin a-associated protein in the endoplasmic reticulum (Fragment)	1.642
B7PPM4	Histone-lysine N-methyltransferase, setb1, putative	1.608
B7Q032	Uncharacterized protein	1.583
A0A4D5RJ63	Putative muscle m-line assembly protein unc-89	1.583
B7Q8I4	CABIT domain-containing protein	1.543
A0A4D5RSN5	Uncharacterized protein (Fragment)	1.514
A0A4D5RRR3	Tetraspanin	1.508
A0A4D5RYS5	Putative peritrophic membrane chitin binding protein (Fragment)	1.506
B7Q2X5	Phosphoinositol 4-phosphate adaptor protein, putative	1.503
B7PPE2	Tnf receptor associated factor, putative (Fragment)	1.498
A0A4D5RIC5	Putative zinc carboxypeptidase (Fragment)	0.664
A0A4D5RLP0	Putative cholesterol transport protein	0.662
A0A4D5RRJ5	Glutathione peroxidase (Fragment)	0.661
B7QKS2	Ig-like domain-containing protein	0.659
B7PQX5	Secreted protein, putative	0.658
B7Q725	Fatty acid synthase, putative	0.656
A0A4D5RHR2	Putative salivary gland secreted protein (Fragment)	0.655
B7PTA2	Cation-transporting ATPase 13a1, putative	0.649
A0A4D5RHF7	Putative gamma-butyrobetaine2-oxoglutarate dioxygenase (Fragment)	0.649
A0A4D5RSQ0	EF-hand domain-containing protein	0.649

B7PQQ9	Selenium-binding protein, putative (Fragment)	0.646
B7PLT0	Secreted protein, putative	0.645
B7P5L3	Nymphal histamine binding protein B, putative (Fragment	0.641
B7PSV2	Methyltransf_11 domain-containing protein	0.638
B7PB63	Leucine-rich transmembrane protein, putative	0.635
B7QA81	Cytochrome P450, putative (Fragment)	0.627
A0A4D5RQM6	Putative hyaluronan mediated motility receptor (Fragment)	0.625
A0A4D5S320	Putative nicotinamide n-methyltransferase (Fragment)	0.621
A0A4D5RFS7	Putative dehydrogenase (Fragment)	0.621
A0A4D5RWS9	Putative secreted protein (Fragment)	0.612
B7Q2V4	Glycine N-methyltransferase, putative	0.605
B7PJA0	Secreted protein, putative	0.604
A0A4D5RMJ7	Putative tick serine proteinase (Fragment)	0.602
Q8MVB9	Uncharacterized protein	0.601
A0A4D5RLW3	Putative secreted protein	0.599
B7QC78	Uncharacterized protein	0.594
A0A4D5RUS6	Putative sulfotransferase	0.591
A0A4D5RNM8	Putative gamma-butyrobetaine2-oxoglutarate dioxygenase (Fragment)	0.588
A0A4D5RT56	Putative serine proteinase inhibitor serpin-3 (Fragment)	0.569
B7QF31	Caspase, apoptotic cysteine protease, putative (Fragment)	0.56
B7PFB3	N-methyltransferase, putative (Fragment)	0.554
B7QNY6	Serine proteinase inhibitor serpin-3, putative	0.55
A0A4D5RQP0	Putative conserved secreted protein (Fragment)	0.535
B7QJY6	Sulfotransferase, putative	0.508
B7PQX7	Uncharacterized protein	0.479
A0A4D5RS70	Putative sulfotransferase (Fragment)	0.479
A0A4D5RPX9	Putative o-methyltransferase (Fragment)	0.468
A0A4D5SAY3	Putative fatty acid synthase (Fragment)	0.458
B7P3V7	Uncharacterized protein	0.446
A0A4D5RUL4	Putative serine proteinase inhibitor	0.395

Table S4: **Differentially produced proteins between *B. burgdorferi*-infected *Dome1*-knockdown and naïve *Dome1*-knockdown ticks**

Accession number	Description	Abundance Ratio (%): (Infected ds*Dome1*) / (Naïve ds*Dome1*)
A0A4D5RHI9	Putative epithelial chloride channel protein	2.108
B7QH07	Cytoplasmic dynein heavy chain, putative	1.969
B7QHR8	Zinc/iron transporter, putative	1.961
A0A4D5RVM4	Putative multiple coagulation factor deficiency 2-like protein (Fragment)	1.856
A0A4D5S3U1	Putative molecular chaperone distantly (Fragment)	1.806
A0A4D5RP87	Uncharacterized protein (Fragment)	1.738
B7Q489	Salivary sulfotransferase, putative	1.734
B7QNV8	Uncharacterized protein	1.732
B7Q2J6	Bis(5'-adenosyl)-triphosphatase	1.643
A0A1S4KT52	WD-repeat protein, putative	1.626
B7QLX7	Uncharacterized protein	1.626
A0A4D5RWJ3	Uncharacterized protein	1.618
A0A4D5RBQ9	Ig-like domain-containing protein	1.617
A0A4D5S513	Putative tumor necrosis factor-alpha-converting enzyme tace/adam17	1.584
A0A4D5RS29	Putative atp-dependent rna helicase (Fragment)	1.578
A0A4D5RRR3	Tetraspanin	1.565
A0A4D5RU19	Putative nucleolar and coiled-body phosphoprotein 1 (Fragment)	1.558
B7QM70	Small heat shock protein, putative (Fragment)	1.554
M4PN64	Cytochrome c oxidase subunit 1 (Fragment)	1.546
B7Q0I5	Proteasome, subunit beta, putative	1.539
B7PQ21	DEAD box ATP-dependent RNA helicase, putative (Fragment)	1.531
A0A4D5RNR7	Putative cytochrome	1.513
B7QL34	Secreted salivary gland peptide, putative	0.669
A0A088CQT2	Cytochrome c oxidase subunit 1 (Fragment)	0.668
A0A4D5RPP1	Putative cytotoxin (Fragment)	0.666
B7Q2V4	Glycine N-methyltransferase, putative	0.666
A0A4D5RRJ4	Putative lysosomal trafficking regulator	0.664
A0A4D5RBB9	Putative chitinase	0.662
A0A4D5RP33	Putative peritrophic membrane chitin binding protein	0.658

B7PXA4	Ves G 1 allergen precursor, putative (Fragment)	0.658
B7PN67	Secreted protein, putative	0.657
Q95WZ0	25 kDa salivary gland protein B	0.656
B7PKZ0	Secreted cystatin, putative	0.656
A0A4D5RS25	Putative rna polymerase-associated protein ctr9 (Fragment)	0.654
A0A4D5S7Q5	Putative cystatin iscys1	0.654
B7PQ15	Niemann-Pick type C1 domain-containing protein, putative	0.653
B7PBU8	Apoptosis-promoting RNA-binding protein TIA-1/TIAR, putative	0.653
B7Q2W4	RAS-related protein, putative (Fragment)	0.647
A0A4D5RGQ6	Putative serine proteinase inhibitor	0.645
A0A4D5RM39	Putative alpha-macroglobulin	0.644
A0A4D5RTY6	Putative rna polymerase ii c-terminal domain-binding protein ra4 (Fragment)	0.641
A0A4D5RG93	Putative trypsin-like serine protease	0.64
B7PIB2	DNA-directed RNA polymerase III subunit RPC5, putative	0.639
A0A4D5RKE2	Putative cytochrome (Fragment)	0.639
A0A4D5RNJ6	Putative serine protease	0.639
A0A4D5RLW3	Putative secreted protein	0.639
A0A4D5RJW4	Putative phd finger protein (Fragment)	0.637
B7QP27	Peptidase, putative	0.637
A0A4D5RVL2	Putative secreted protein (Fragment)	0.637
A0A4D5RFM0	Putative serine protease (Fragment)	0.636
B7PIV2	Uncharacterized protein	0.634
B7PKG2	Fasciclin domain-containing protein, putative	0.634
B7Q911	tRNA pseudouridine synthase	0.633
B7PW73	Transcription initiation factor TFIID subunit 10	0.632
B7QKR7	Secreted protein, putative	0.632
B7P7W6	Innexin	0.631
B7QNH1	Triacylglycerol lipase, putative (Fragment)	0.629
B7Q8R2	Pyrroline-5-carboxylate reductase 1	0.629
Q5ISE3	Scapularisin preproprotein	0.628
A0A4D5RLH7	Putative 4-hydroxyphenylpyruvate dioxygenase (Fragment)	0.625
A0A4D5RKR3	Putative cytochrome (Fragment)	0.625
B7QDU9	DUF3421 domain-containing protein	0.624
A0A4D5RG89	Putative focal adhesion adaptor protein paxillin (Fragment)	0.62
A0A4D5SB53	Putative conserved secreted protein	0.619

A0A4D5S4Y8	Phospholipase B-like (Fragment)	0.618
B7P5K8	Branched-chain amino acid aminotransferase, putative	0.618
B7QIK8	Chitinase, putative	0.618
A0A4D5RFD8	Putative serine protease	0.616
B7Q1Z5	Uncharacterized protein	0.615
A0A4D5RJJ4	Putative sulfotransferase	0.612
A0A4D5S6D9	Putative paramyosin (Fragment)	0.612
B7Q4V8	Uncharacterized protein	0.612
A0A4D5S3C6	Putative tp53-induced glycolysis and apoptosis regulator b (Fragment)	0.611
B7QMM1	Glycine C-acetyltransferase/2-amino-3-ketobutyrate-CoA ligase, putative (Fragment)	0.61
B7PLJ7	Apoptosis inducing factor, putative	0.61
A0A4D5RFD3	Putative serine proteinase 2	0.609
B7PA38	Peptidyl-prolyl cis-trans isomerase E	0.609
B7P370	Ferrochelatase	0.607
B7PPW4	PRA1 family protein	0.607
A0A4D5RJV0	Putative transcription factor (Fragment)	0.607
A0A4D5S1S8	Putative paramyosin (Fragment)	0.606
A0A4D5RPJ8	Putative serine proteinase	0.606
B7PH24	Serine protease inhibitor, putative	0.606
B7PN60	Esterase, putative (Fragment)	0.606
A0A4D5RG65	Putative membrane glycoprotein lig-1	0.605
A0A4D5RL78	Putative 15-hydroxyprostaglandin dehydrogenase (Fragment)	0.604
B7PNJ5	Serine proteinase inhibitor, putative	0.602
A0A4D5RG19	Putative ml domain protein	0.601
A0A4D5RKG9	Putative abl interactor abi-1 (Fragment)	0.599
B7Q2X5	Phosphoinositol 4-phosphate adaptor protein, putative	0.597
B7Q135	Secreted protein, putative	0.596
A0A4D5RRT2	Putative mitochondrial/plastidial beta-ketoacyl-acp reductase (Fragment)	0.596
B7PV75	Glutathione peroxidase	0.595
B7PLF9	Kinesin-associated protein, putative	0.594
B7QL39	Translation elongation factor G, putative (Fragment)	0.593
B7Q9Y6	Rif1_N domain-containing protein	0.593
B7QIW2	Secreted salivary gland peptide, putative	0.593
A0A4D5RKW6	Putative l-threonine 3-dehydrogenase mitochondrial-like protein (Fragment)	0.592

A0A4D5S2K3	Putative single domain von willebrand factor type c (Fragment)	0.592
B7QF31	Caspase, apoptotic cysteine protease, putative (Fragment)	0.592
A0A4D5RUP4	Putative gastric triacylglycerol lipase	0.589
B7PY78	DNA-repair protein xrcc1, putative (Fragment)	0.589
B7PZH4	Animal-type fatty acid synthase, putative	0.585
B7PFI1	Molybdenum cofactor biosynthesis pathway protein, putative	0.585
A0A4D5RQW5	Putative membrane glycoprotein lig-1	0.584
B7P102	Membrane glycoprotein lig1, putative	0.584
A0A4D5REU5	Putative pancreatic lipase-like enzyme (Fragment)	0.583
B7PCM5	Uncharacterized protein	0.582
B7PYG8	Secreted salivary gland peptide, putative	0.582
A0A4D5S4X0	Putative epithelin/granulin (Fragment)	0.58
A0A4D5RK10	Putative membrane glycoprotein lig-1	0.579
A0A4D5RWS9	Putative secreted protein (Fragment)	0.578
B7PQX7	Uncharacterized protein	0.577
B7PMF3	Secreted protein, putative	0.575
B7PTS6	AAA domain-containing protein	0.574
B7PSK7	Alanine-glyoxylate aminotransferase, putative	0.573
A0A4D5S4H2	Putative acetylcholinesterase/butyrylcholinesterase (Fragment)	0.573
A0A4D5S320	Putative nicotinamide n-methyltransferase (Fragment)	0.573
B7PS56	Secreted salivary gland peptide, putative	0.571
B7Q2Y8	Secreted salivary gland peptide, putative	0.571
B7QKG0	ACB domain-containing protein	0.57
A0A4D5RZ46	Putative non-muscle myosin heavy chain ii	0.568
A0A4D5RTN0	Putative membrane protein	0.568
B7QC78	Uncharacterized protein	0.568
B7P7L1	Uncharacterized protein	0.567
B7QCM5	Ribose-5-phosphate isomerase, putative (Fragment)	0.565
B7PG23	Serine proteinase inhibitor, putative	0.564
B7PS64	Cytochrome P450, putative (Fragment)	0.562
B7PBF8	ADP ribosylation factor 79F, putative (Fragment)	0.559
B7PQ22	Crystal protein, putative	0.559

A0A4D5RT56	Putative serine proteinase inhibitor serpin-3 (Fragment)	0.559
A0A4D5RTF2	Uncharacterized protein (Fragment)	0.558
B7P2U1	Uncharacterized protein	0.556
A0A4D5RLC8	Putative catalytic domain of phosphatidylinositol-specific phospholipase c x domain protein	0.556
A0A4D5RJD5	Putative notch signaling protein (Fragment)	0.554
A0A4D5RPH6	Putative copper-transporting atpase 1	0.554
A0A4D5S005	Putative chitinase (Fragment)	0.554
A0A4D5REA9	Glucose-6-phosphate isomerase	0.553
A0A4D5S423	Putative paramyosin	0.55
A0A1S6Y024	Reeler domain-containing gut protein	0.549
A0A4D5S5P0	Uncharacterized protein	0.546
A0A4D5RFC8	Putative histone acetyltransferase saga trrap/tra1 component pi-3 kinase superfamily protein (Fragment)	0.545
B7PLN8	Secreted protein, putative	0.54
A0A4D5RNY4	Glucosylceramidase	0.54
A0A4D5S337	Putative antimicrobial peptide	0.539
B7PTN7	Prolyl 4-hydroxylase alpha subunit, putative (Fragment)	0.539
A0A4D5RPD4	Putative zinc carboxypeptidase (Fragment)	0.538
A0A4D5RGX3	Putative tick serine proteinase (Fragment)	0.537
A0A4D5RFE7	Tubulin gamma chain (Fragment)	0.533
B7PHX3	Chymotrypsin-C precursor, putative	0.533
B7PUZ3	Loss of heterozygosity 12 chromosomal region 1 protein, putative	0.533
B7QGM6	Phospholipase A2 precursor, putative	0.53
B7PAY4	Zinc phosphodiesterase, putative	0.53
B7PLT0	Secreted protein, putative	0.529
A0A4D5S624	Putative serine proteinase (Fragment)	0.528
B7P635	Sulfotransferase, putative	0.527
A0A4D5RVG6	Putative sulfotransferase	0.525
A0A4D5RRW2	Putative transporter (Fragment)	0.525
A0A4D5RUS6	Putative sulfotransferase	0.524
B7Q0W8	39S ribosomal protein L21, putative	0.523
B7PV21	Synaptotagmin-14, putative	0.522
B7QI18	RAB GDP/GTP exchange factor, putative	0.52
B7PUS3	Peroxisomal phytanoyl-CoA hydroxylase, putative	0.518
B7PR40	SCP domain-containing protein	0.515
B7Q725	Fatty acid synthase, putative	0.515

B7PJW5	Peritrophic membrane chitin binding protein, putative	0.514
A0A4D5RX10	Protein disulfide-isomerase	0.511
A0A4D5RQM6	Putative hyaluronan mediated motility receptor (Fragment)	0.511
B7P8V8	Uncharacterized protein	0.509
B7P101	Membrane glycoprotein LIG-1, putative	0.504
A0A1S4M122	Actin, putative	0.502
A0A4D5RJY2	Putative hemolectin (Fragment)	0.499
B7PTA2	Cation-transporting ATPase 13a1, putative	0.496
A0A4D5RDR9	Putative vacuolar assembly/sorting (Fragment)	0.494
A0A4D5RQI3	Putative salivary secreted peptide	0.49
B7Q713	Astacin, putative	0.49
A0A4D5RIY3	Methionine aminopeptidase (Fragment)	0.488
B7PH23	Secreted protein, putative	0.486
B7QKR4	25 kDa salivary gland protein C, putative	0.483
B7QKS2	Ig-like domain-containing protein	0.483
B7PJA0	Secreted protein, putative	0.483
A0A4D5RLH3	Putative pancreatic lipase-like enzyme (Fragment)	0.476
A0A4D5RXM4	Calreticulin	0.476
B7P6U4	Salivary secreted cytotoxin, putative	0.476
B7Q1H6	Laminin gamma-1 chain, putative (Fragment)	0.475
A0A4D5RK09	Putative regulation of transcription (Fragment)	0.473
A0A4D5RMT9	Putative cholesterol transport protein	0.473
A0A4D5RFS7	Putative dehydrogenase (Fragment)	0.473
A0A4D5S7C6	Putative antimicrobial peptide	0.472
B7QJY6	Sulfotransferase, putative	0.471
B7PL51	ML domain-containing protein, putative	0.47
B7P1I0	Titin, putative	0.464
B7P5L3	Nymphal histamine binding protein B, putative (Fragment)	0.458
B7QK00	Uncharacterized protein (Fragment)	0.455
A0A4D5RD42	Putative eukaryotic translation initiation factor 4 gamma 1-like isoform x2 (Fragment)	0.449
B7PTV6	FYVE-type domain-containing protein (Fragment)	0.447
B7PMM4	ABC transporter, putative (Fragment)	0.447
A0A4D5RN87	Putative serine proteinase inhibitor	0.443
A0A4D5RQN5	Putative secreted protein (Fragment)	0.438
A0A4D5RR07	Putative conserved secreted protein	0.435

B7P1I1	Secreted protein, putative (Fragment)	0.435
B7PMM0	Uncharacterized protein	0.424
B7PS13	ING (mammalian INhibitor of Growth) family protein (ing3)-like, putative (Fragment)	0.423
A0A4D5RRJ5	Glutathione peroxidase (Fragment)	0.417
B7QJ79	Replication factor C, subunit RFC2, putative	0.414
Q8MVG3	Putative secreted protein	0.414
A0A4D5S4C3	Uncharacterized protein (Fragment)	0.413
B7PQF4	Sulfotransferase, putative	0.412
B7P9L7	Preprodefensin, putative	0.404
Q4PML3	Putative salivary secreted protein	0.403
A0A4D5RIC5	Putative zinc carboxypeptidase (Fragment)	0.388
Q95WZ5	Histamine binding protein	0.386
B7P1H7	Titin, putative	0.381
B7Q4J7	Glutathione S-transferase, putative	0.378
A0A4D5RLP0	Putative cholesterol transport protein	0.375
A0A4D5RRX9	Putative ml domain protein	0.37
B7Q2B8	Metalloprotease, putative	0.369
B7PUC0	AKAP2_C domain-containing protein	0.36
B7QNS1	Amino acid transporter	0.358
A0A4D5SAY3	Putative fatty acid synthase (Fragment)	0.341
B7PJW6	Chitin deacetylase 9, putative	0.333
Q4PNA3	Putative secreted protein with basic tail	0.33
Q4PMX1	Putative salivary HBP family member	0.323
B7Q8I4	CABIT domain-containing protein	0.321
B7QM92	Peptidase M12B domain-containing protein	0.318
F6KSY1	Salivary protein antigen P8	0.315
B7QFF3	Lipase, putative (Fragment)	0.297
A0A1S4M4I5	Salivary gland metalloprotease, putative	0.296
B7Q0V7	Secreted protein, putative (Fragment)	0.29
A0A4D5RU61	Putative hydroxysteroid 17-beta dehydrogenase 11 (Fragment)	0.287
Q8MVB9	Uncharacterized protein	0.276
B7P1H9	Neurotrimin, putative (Fragment)	0.268
Q5S1X6	Fed tick salivary protein 4	0.266
B7QFI5	Cell adhesion molecule, putative	0.258
B7P3G0	Chitinase, putative (Fragment)	0.256
B7PYE3	Secreted salivary gland peptide, putative (Fragment)	0.242
B7Q2C1	Metalloprotease, putative	0.237
A0A4D5S4Q9	Putative salivary protein with polyk tail	0.237
A0A4D5RAJ8	Putative secreted metalloprotease	0.221
Q8MVB0	Truncated secreted metalloprotease	0.204

Table S5: **Culture analysis of murine tissues engorged by infected ticks**

Isolation of viable *B. burgdorferi* by culture analysis of tissues from murine hosts after infestation with control (ds*GFP*) or various knockdown ticks (ds*Dome1*, ds*JAK*, and ds*STAT*), as detailed in the manuscript, is shown. The culture positivity or negativity of each tissue type from each individual animal (four mice per group) is indicated by "+" or "-", respectively.

	Skin	**Heart**	**Joint**
ds*GFP*	+ + + +	+ - - -	+ + + +
ds*Dome1*	- - - -	- - - -	- - - -
ds*JAK*	+ - - +	- - - -	- - - -
ds*STAT*	- - - -	- - - -	- - - -

Table S6: **Oligonucleotide primers used in the study (FP, forward primer; RP reverse primer)**

Primer name	5′-sequence-3′	Purpose
Dome1 pcDNA FP	GACTACAAAGACGATGACGACAAGGCCTGC CGTTCTATCTTCTCTCCCATC	EC expression (CHO)
Dome1 pcDNA His RP	GACACTATAGAATAGCTAATGATGATGATGA TGATGTGAGATGGCGGGACCAACAGACTC	EC expression (CHO)
Dome1 pGEX1 FP	GGTGAATTCATGAACAAGACGTCCCTGATG G	Truncated EC expression (*E. coli*)
Dome1 pGEX1 RP	GGTGGTGCGGCCGCTTGGAAACTGGGATC ACACA	Truncated EC expression (*E. coli*)
Dome1 IG FP	ACATGGATCCGCCTGCCGTTCTATCTTCTCT CCCATC	IG domain expression (*E. coli*)
Dome1 IG RP	TAGTGTCGACTCATCCGACGGTGACTAACG TTGC	IG domain expression (*E. coli*)
GFP RNAi 1FP	AATGAGCTCGAGGTGAAGTTCGAGGGCGA	RNA interference (RNAi)
GFP RNAi 1RP	AATGGTACCTCCATGCCGAGAGTGATCCC	RNAi
Dome1 RNAi 1FP	TAATACGACTCACTATAGGGGTGCCAGATTC GCCACCTA	RNAi
Dome1 RNAi 1RP	TAATACGACTCACTATAGGGCAGAACACTGT GTAGCCTGG	RNAi
Dome1 RNAi 2FP	TAATACGACTCACTATAGGGGCATGCTGCC CCGTTCGTA	RNAi
Dome1 RNAi 2RP	TAATACGACTCACTATAGGGCCGGTAGACC GAGTTTGTGT	RNAi
Dome1 RNAi 3FP	TAATACGACTCACTATAGGGCTCATTGGTCA TTGGAGTGG	RNAi
Dome1 RNAi 3RP	TAATACGACTCACTATAGGGGAGGCTGTCG TGGCCGTT	RNAi
Dome1 RNAi 4FP	TAATACGACTCACTATAGGGGTCCTCCCTAC CCACAACAC	RNAi
Dome1 RNAi 4RP	TAATACGACTCACTATAGGGGACCGACACA CGGAGTACG	RNAi
Dome1 RNAi 5FP	TAATACGACTCACTATAGGGGAGTCCCACC CTTTTTGGG	RNAi
Dome1 RNAi 5RP	TAATACGACTCACTATAGGGTAAACAGTCGG CGGGTTCA	RNAi
Dome1 QFP	TGGACTGAGAGCGTCTTCCT	Quantitative PCR (qPCR)
Dome1 QRP	CACCTGTCCTCCAGTGGATT	qPCR
Dome2 Q FP	CGATGATCTTCGTCAAAGCA	qPCR
Dome2 Q RP	TTTCAACAGAGCGGAGGAGT	qPCR
Dome3 Q FP	ATGACCGATCAGACTGAGTCTCAAGAC	qPCR
Dome3 Q RP	CTCGTACAAGATATCCGGGAACG	qPCR
Dome4 Q FP	GCCAACACAGAGTTCGAGGT	qPCR
Dome4 Q RP	CCACAGAGTTCTTGCTCGTG	qPCR
Dome5 Q FP	ACTCAAGCCCTTTTCGTTCTACG	qPCR
Dome5 Q RP	TGTGGTCGCTCCCATTGTAGG	qPCR
Dome5 RNAi 1FP	TAATACGACTCACTATAGGGCGTCATCCTGC ACTACATC	RNAi

Dome5 RNAi 1RP	TAATACGACTCACTATAGGAGGTATTGGGTAAAGGTTTCC	RNAi
Dome5 RNAi 2FP	TAATACGACTCACTATAGGCTGTACGAGGTGAAGGTGCAG	RNAi
Dome5 RNAi 2RP	TAATACGACTCACTATAGGAGGCTTGTTCTCGTTCAGTTG	RNAi
Dome5 RNAi 3FP	TAATACGACTCACTATAGGGGTGTACCAGTATCACTACAC	RNAi
Dome5 RNAi 3RP	TAATACGACTCACTATAGGATCGGTTCTTTGCCTTGTTGC	RNAi
Dome5 FP	ATTCAGATCTGTTCCCGACCCCCCGGGGATCCCCATCGTG	Protein expression (*E. coli*)
Dome5 RP	ATAGCTCGAGTTACTCTGACACTTACTCTGAAGG	Protein expression (*E. coli*)
B. burgdorferi flaB FP	TTGCTGATCAAGCTCAATATAACCA	qPCR
B. burgdorferi flaB RP	TTGAGACCCTGAAAGTGATGC	qPCR
Staphylococcus 16 QFP	CGGACGAGAAGCTTGCTT	qPCR
Staphylococcus 16 QRP	GCATCGTTGCCTTGGTA	qPCR
Acinetobacter 16s Q FP	TAGAGTATGGGAGAGGA	qPCR
Acinetobacter 16s Q RP	TTTACGGCATGGACTACC	qPCR
Pseudomonas 16s Q FP	TGCTGAGAACTTTCCAGAGA	qPCR
Pseudomonas 16s Q RP	GCTAAGGGCCATGATGAACTT	qPCR
Enterococcus 16s Q FP	CCTGCCCATCAGAAGGG	qPCR
Enterococcus 16s QRP	CCTGTCTCAGTCCCAATGTGGCCGATCACC	qPCR
Rickettsia 16s Q RP	CTTGCGTTAGCTCACCACCT	qPCR
Rickettsia 16s Q FP	CGTGGAGCAAATCCCTAAAA	qPCR
Lysinibacillus 16s Q FP	CGCGAGAGGGAGCTAATCCGATAAAG	qPCR
Lysinibacillus 16s Q RP	CTATCCCACCTTCGGCGGCTGGCTCCAA	qPCR
Brevibacterium 16s Q FP	CGTCTGCTGTGGAAACGCAA	qPCR
Brevibacterium 16s Q RP	CCTTGGTAAGGTTCTTCG	qPCR
Protein Kinase C Q FP	TTCTGCGTCGTCAACCTCAAGG	qPCR
Protein Kinase C Q RP	CTCGTAGATCTTCTGGTGCTTGATG	qPCR
Peroxiredoxin Q FP	CAAAGGCCAAGTACCACCTCAAG	qPCR
Peroxiredoxin Q RP	GCTTGTTCGGATGGGTTGTGG	qPCR
Glutathione peroxidase Q FP	GGAGATTCTGAACGGGATCAAGTACG	qPCR

Glutathione peroxidase Q RP	GCCTGTCAACCAGAAACTTCTCG	qPCR
*Peritrophin-1*FP	ATGCCGAATAAGGTCGACTG	qPCR
*Peritrophin-1*RP	AGTGGAATCTGGACGGAATG	qPCR
*Peritrophin-2*FP	AGAAGGGATTGGCCTTCAAC	qPCR
*Peritrophin-2*RP	TACAGGCTACGCAACAAACG	qPCR
*Peritrophin-3*FP	TGTGACAAGACGACCTCCAG	qPCR
*Peritrophin-3*RP	CATCGAGTTCTTGGCCTGT	qPCR
*Peritrophin-4*FP	ACCTGTCGACGGATGTGACT	qPCR
*Peritrophin-4*RP	CCTCGCACGTGTAGCTGTAG	qPCR
*Peritrophin-5*FP	ACCTGGGATTCCAGTGTCC	qPCR
*Peritrophin-5*RP	CCAGCCGTGCACGTTGAG	qPCR
JAK RNAi FP	TAATACGACTCACTATAGGGACTCTGGATAG GATTAAGG	RNAi
JAK RNAi RP	TAATACGACTCACTATAGGGCAAGTGATGCT CTCTTTG	RNAi
Mouse *Actb* QFP	AGAGGGAAATCGTGCGTGAC	qPCR
Mouse *Actb* QRP	CAATAGTGATGACCTGGCCGT	qPCR
I. scapularis Actb QFP	GGTATCGTGCTCGACTC	qPCR
I. scapularis Actb QRP	ATCAGGTAGTCGGTCAGG	qPCR
Notch Q FP	CGTCACCCTCGACAACTACACG	qPCR
Notch Q RP	CTCGCAGGGCTTTGCCTTGC	qPCR
Delta Q FP	CGCGGACTTTGAATCGGTTG	qPCR
Delta Q RP	TGACGTAGACGACCGAACTG	qPCR
Hedgehog QFP	GGAGGTGATCAGCTTCTTGGATCG	qPCR
Hedgehog QRP	GGTACTAGTCTGCACCAGAATGTAGC	qPCR
Hedgehog RNAi FP	TAATACGACTCACTATAGGGGTTCCACAGAT GGCGCTTCC	RNAi
Hedgehog RNAi RP	TAATACGACTCACTATAGGGTCAGTCCAGAA GATACGACT	RNAi
EGF Q FP	TTCAGAACAAGAGCCTGGACCTGAG	qPCR
EGF Q RP	CAGGTTGTCCATCTTGCTCAGGGTG	qPCR
*Hox1*Q FP	CAGACAAACGCTGCGGGTGAAC	qPCR
*Hox1*Q RP	TGCGTCTGCGTGAGACCGAG	qPCR
*Hox2*Q FP	GATTTTTTGCTCCCCTTCCCCTCG	qPCR
*Hox2*Q RP	AGGGTCTGGAACTTAGAGTAAGGTTTACG	qPCR
*Hox 3*Q FP	TCTAGCGACGCTAGCACAAAGAGG	qPCR
*Hox3*Q RP	TGTCCCACATGGCTTCATTTGTACC	qPCR
*Hox4*Q FP	CTTCCAAAGCTGGTGCCCTCTGG	qPCR
*Hox4*Q RP	CAGGTAGTGGTTCGTGTGGAACTCC	qPCR
*Hox5*Q FP	GACATCGATATCGCCATGAGCTCG	qPCR
*Hox5*Q RP	CAGCCTATCATACGGCGGAAACC	qPCR
*Hox7*Q FP	GACCCTGGAGTTGGAGAAAGAGTTCC	qPCR
*Hox7*Q RP	TTGGCCATCTTGTGCTCCTTCTTCC	qPCR
*Hox8*Q FP	CAGATCCTTGAGCTGGAGAAAGAGTTCC	qPCR
*Hox8*Q RP	TTGTCCTTCTTCCACTTCATGCGTCG	qPCR
*Hox9*Q FP	CTGCCGTTTCTACCGATGCTCCTC	qPCR
*Hox9*Q RP	AAGGCTCCCTGCTCGTCTTG	qPCR

Uni *Dome1* QFP	CCAGCACTTCCCTACTCCCAGC	qPCR (*Dermacentor variabilis*)
Uni *Dome1* QRP	GCTGGGTCTTCATGGCTTGC	qPCR (*D. variabilis)*
Uni *Dome1* RNAi FP	TAA TAC GAC TCA CTA TAG GGC GGG CAA CTA CAA CTG CAA C	RNAi (*D. variabilis)*
Uni *Dome1* RNAi RP	TAA TAC GAC TCA CTA TAG GTG CGA CGT CTT GTT GAA CAC C	RNAi (*D. variabilis)*
Dome1 Uni 1 FP	ATT CGG ACA CGG GCA ACT ACA ACT GCA AC	Cloning of Dome1 ortholog (*D. variabilis)*
Dome1 Uni 1 RP	TCT GAT AAT TCT GCA CCT TGA AGC C	Cloning of Dome1 ortholog (*D. variabilis)*
Dome1 Uni 2 FP	GTG AGC TAC ACG GTG TTC TGG TG	Cloning of Dome1 ortholog (*D. variabilis)*
Dome1 Uni 2 RP	GTC AGC GGC AGA AAA GCA GCC CAT C	Cloning of Dome1 ortholog (*D. variabilis)*
Dome1 Full FP	ATG GAC GGG AGG CAA TGG CGG CAC C	Cloning of Dome1 ortholog (*D. variabilis)*
Dome Full RP	TCA CAC CGA GCA GTC CAC	Cloning of Dome1 ortholog (*D. variabilis)*
DvAct1424F QFP	CTTTGTTTTCCCGAGCAGAG	qPCR of *D. variabilis*
DvAct1424F QRP	CCAGGGCAGTAGAAGACGAG	qPCR of *D. variabilis*
Aa Actb Q FP	TCCTATCCTCACCCTGAAGTA	qPCR of *Amblyomma americanum*
Aa Actb Q RP	ACGCAGCTCGTTGTACAAG	qPCR of *A. americanum*

Table S7: Details of antibodies used in the study

Antibodies	Reference number, Source	Clone number	Dilution
Anti-Dome 1 (Truncated EC) antibody	Current study		IF- 1:100
Anti-Dome 1 (IG domain) antibody	Current study		WB- 1:3000
Anti-Dome 5 antibody	Current study		WB- 1:2000
Phospho-Histone H3(Ser10) antibody	9701S, Cell Signaling Technology Inc.		IF- 1:100
IFN gamma monoclonal antibody Host: Rat, species reactivity : Mouse	14-7312-85, Thermo Fisher Scientific	R4-6A2	IF- 1:150 ELISA- 1:1000
Anti- chicken IFN gamma Polyclonal Antibody, Host: Rabbit	PB0442C-100 Kingfisher Biotech Inc.		ELISA- 1:1000
Purified anti-human IFN-γ Antibody, Host: Mouse	502501, BioLegend Inc.	4S.B3	ELISA- 1:1000
Alexa Fluor 488 goat anti-rabbit	A-11008 Thermo Fisher Scientific		IF- 1:150
Alexa Fluor 568 goat anti-rat	A-11077, Thermo Fisher Scientific		IF- 1:150
Phospho-STAT5 alpha (Tyr694) Polyclonal antibody Host: Rabbit	71-6900, Thermo Fisher Scientific		WB- 1:1000
FITC conjugated goat anti *Borrelia* Antibody Host: Rabbit	95058-200, VWR International LLC.		IF- 1:200
Goat Anti Mouse HRP conjugate antibody	5220-0341, Sera Care		WB- 1:10000 ELISA- 1:1000
Goat Anti-Rabbit IgG-HRP antibody	4030-05 SouthernBiotech		WB- 1:4000 ELISA- 1:1000
Goat Anti-Rat IgG-HRP antibody	14-16-12 Kirkegaard &Perry Laboratories		WB- 1:10000 ELISA- 1: 1000
Anti-DDDDK tag antibody Host: Rabbit	ab 1162, Abcam		WB- 1: 3000

WB- Western blotting, **IF**- Immunofluorescence assay, **ELISA-** Enzyme-linked immunosorbent assay

Table S8: **Protein accession numbers used for the construction of phylogenetic trees**

Figure number(s)	Accession numbers
1C	Dome1 (*Ixodes scapularis*, XP_029844458.1) IFNGR (*Mus musculus*, NP_034641.1) IFNGR 1 (*Homo sapiens*, NP_000407.1) IFNGR 2 (*Homo sapiens*, NP_001316057.1)
1B and 1D	IFNGR1 (*Rattus rattus*, XP_032750830.1) IFNGR1 (*Homo sapiens*, NP_000407.1) IFNGR1 (*Mus musculus*, NP_034641.1) Cnftr (*Homo sapiens*, NP_001833.1) Cnftr (*Mus musculus*, AAH50928.1) IL6 (*Rattus norvegicus*, NP_058716.2) IL6 (*Homo sapiens*, NP_00556.1) Arthropod Dome ectodomain orthologs: *Bombyx mori*, XP_012546276.2; *Drosophila melanogaster*, NP_523412.1; *Musca domestica*, XP_005192086.1; *Cimex lectularius*, CLEC012032; *Aedes aegypti*, XP_001662596.2; *Melipona quadrifasciata*, KOX70826.1; *Cherax quadricarinatus*, QKU38106.1; *Eriocheir sinensis*, QBA18592.1; *Penaeus vannamei*, AGY46351.1;*Strigamia maritima,* SMAR011060-RA, SMAR011063-RA;*Ixodes scapularis*, XP_029844458.1; *Dermacentor silvarum,* XP_037556658.1; *Rhipicephalus microplus,* XP_037287858.1; *Galendromus occidentalis*, XP_003744080.1; *Sarcoptes scabiei*, KAF7491423.1; *Parasteatoda tepidariorum*, XP_015924832.1; *Dinothrombium tinctorium*, RWS16955.1; *Tetranychus urticae*, XP_025016179.1
S3	Interfer-bind motif: Uncharacterized protein (*Nocardioides albidus*, A0A5C4VQX2/73-161) FNIII (*Roseburia sp.*, R5UNT6/34-137) Uncharacterized protein (*Winogradskyella epiphytica*, A0A0A1DVD9/41-134) FNIII protein (*Anaerostipes sp.*, R6QE57/57-116 protein) Dome1 (*Ixodes scapularis*, XP_029844458.1/255-321) Secreted protein (*Arthrobacter simplex*, A0A2V4XIC5/317-366) Endonuclease I (*Xanthomarina gelatinilytica*, M7MET9/309-367) Cytokine Receptor family (*Danio rerio*, A0FJH7_DANRE/115-217) IFN bind domain containing protein (*Tetraodon nigroviridis*, H3C2Q6_TETNG/53-151) IFNgR 2 (*Bos taurus*, INAR2_BOVIN/132-234)

	FNIII (*Amycolatopsis sulphurea*, A0A2A9FF12/102-196) IFNgR 2 (*Homo sapiens*, NP001316057.1) IFNAR1 (*Gallus gallus*, A0A1D5PRB3_CHICK/133-231) IFNAR1 (*Sus scrofa*, INAR1_PIG/125-224) IFNgR (*Mus musculus*, NP_034641.1/132-244) IFNgR 1 (*Homo sapiens*, NP_000407.1/126-237) Tissue Factor (*Sumatran orangutan*, Q5R8A6_PONAB/138-245) LacI (*Rattus norvegicus*, Q66HI4_RAT/139-246) Tissue Factor (*Oryctolagus cuniculus*, TF_RABIT/136-243) Interferon alpha/beta receptor 1 (*Bos taurus*, INAR1_BOVIN/330-431) Dome1/Cytokine Receptor: IFNGR2 (*Pantherophis guttatus*, XP_034291103.1) IFNGR2 (*Ophiophagus hannah*, ETE58933.1) IFNGR2 (*Thamnophis elegans*, XP_032075387.1) IFNGR2 (*Lacerta agilis*, XP_033002843.1) IFNGR2 (*Anolis carolinensis*, AGL76447.1) IFNGR2 (*Sceloporus undulatus*, XP_042315051.1) IFNGR2 (*Aquila chrysaetos*, XP_029876211.1) IFNGR2 precursor (*Gallus gallus*, NP_001008676.2) CIB84_003046 (*Bambusicola thoracicus*, POI33204.1) IFNGR2 (*Lagopus leucura*, XP_042722314.1) IFNGR2 precursor (*Mus musculus*, NP_032364.1) LIFR (*Homo sapiens*, NP_002301.1) Cytokine receptor (*Musca domestica*, XP_005192086.1) Cytokine receptor NR10 (*Mus musculus*, BAB88745.1) Dome1 (*Ixodes scapularis*, XP_029844458.1) Ortholog Dome (*Dermacentor silvarum*, XP_037556658.1) Ortholog (*Rhipicephalus microplus*, XP_037287858.1) Cytokine receptor (*Homo sapiens*, AAA93193.1) Cntfr protein (*Mus musculus*, AAH50928.1) CNFTR (*Homo sapiens*, NP_001833.1) CNFTR X1 (*Homo sapiens*, XP_016869749.1)
S18	Dome orthologs *Hyalomma asiaticum*, DKAH6941609.1; *Rhipicephalus microplus*, XP_037287858.1; *Rhipicephalus sanguineus*, XP_037527344.1; *Haemaphysalis longicornis*, KAH9366377.1; *Dermacentor silvarum*, XP_037556658.1; *Dermacentor variabilis*, OP503541; *Ixodes scapularis*, XP_029844458.1